

Vol. 10. Issue 2, 2024

ISSN: 2453-7314

Central European Researchers Journal



A WORD OF WELCOME FROM THE EDITORS

Dear Colleagues, Readers and Authors,

We are pleased to present the year-end issue of our journal, bringing you the latest trends, research and achievements in the field of technical cybernetics. In this special issue, we bring you a diverse selection of articles that reflect the advances and innovative projects in this dynamic field.

Among the most interesting contributions is an article on measuring kinetic energy from wind-induced tree movement, which demonstrates the potential of renewable energy sources. Another important project is the use of artificial intelligence in the measurement and processing of muscle signals, which opens up new possibilities in biomedical engineering. You will also be interested in the analysis of the sustainability of the 3D printing lab's operations, which shows how modern technologies can be greener and more efficient.

This issue also highlights the active involvement of students in several projects, underlining their important role in research and development. Their contribution is particularly visible in the innovative solutions that not only develop their professional skills but also contribute to the advancement of the entire field.

The vision of this journal is to provide information that is not only valuable but also beneficial to all those interested in advances in cybernetics. We hope that this issue will provide you with a rich source of knowledge and new perspectives. If you have suggestions, comments, or ideas for improvement, we cordially invite you to share them with us.

I wish you a pleasant reading and many inspiring insights!

Sincerely,

The Editorial Team

Central European Researchers Journal. Volume 10. Issue 2

Editor-in-chief: Kharchenko Vyacheslav, Zaitseva Elena

Editorial Board: Androulidakis Iosif, Belotserkovsky Alexei, Bezobrazov Sergei, Cariow Aleksandr, Cimrak Ivan, Dmytrychenko Mykola, Drahansky Martin, Drozd Alexander, Frenkel Ilia, Filatova Darya, Kachurka Pavel, Khakhomov Sergei, Kor Ah-Lian, Koshkin Gennady, Lapitskaya Natalia, Levashenko Vitaly, Liauchuk Viktor, Lukac Martin, Lukashevich Marina, Matiasko Karol, Melnychenko Oleksandr, Oliinyk Andrii, Pancierz Krzysztof, Slavinskaya Elena, Stankevich Sergey, Subbotin Sergey, Tatur Michail, Vojnar Tomas, Volochiy Bogdan, Yakovyna Vitaliy, Zhivitskaya Helena.

Address of the editorial office: Central European Researchers Journal - editorial, Faculty of Management Science and Informatics, University of Zilina, Univerzita 8215/1, 01026, Zilina, Slovakia, editorial@ceres-journal.eu

Each paper was reviewed by reviewers.

Publisher: JMTM, s.r.o., Sad SNP 8, 010 01, Zilina, Slovakia, publisher@jmtm.sk

Published biannually

ISSN: 2453-7314

December 2024

CONTENTS

| | |
|--|----|
| <i>Ondrej Karpiš, Tomáš Bača, Ján Šumský, Michal Kubaščík</i> Support for Teaching the Subject Digital Computers | 1 |
| <i>Tomáš Bača, Ján Šumský, Michal Kubaščík, Peter Šarafín</i> Measuring Kinetic Energy from Tree Movements Induced by Wind | 6 |
| <i>Richard Bořanský, Michal Hodoň, Lukáš Čechovič, Peter Ševčík</i> Universal System for Indoor Location | 16 |
| <i>Adrián Hložný, Michal Hodoň, Lukáš Formanek</i> Wireless Voting System | 19 |
| <i>Martin Uhrina, Michal Kubaščík, Ján Kapitulík</i> Measurement of Muscle Signals and their Processing Using AI | 23 |
| <i>Miloslav Slodičák, Michal Hodoň, Juraj Miček, Peter Ševčík</i> System for Quality of Traffic Infrastructure Measurements | 28 |
| <i>Lukáš Čechovič, Marek Tebeľák, Michal Kubaščík, Juraj Miček</i> Sustainability of the 3D Printing Laboratory Operation on Faculty of Management Science and Informatics University of Žilina | 33 |
| <i>Tomáš Bača, Marek Tebeľák, Michal Kubaščík, Juraj Miček</i> Design and Implementation of a Light Information Panel for Safety Car | 39 |
| <i>Lukáš Čechovič, Andrej Tupý, Marek Tebeľák, Juraj Miček</i> The Effect of High-Pressure Cooling Systems in FDM 3D Printers on VOC and PM Emissions | 44 |
| <i>Ivan Stankovský, Michal Hodoň, Peter Ševčík</i> Automatic Coin Sorting Machine | 49 |
| <i>Patrik Ivan, Michal Hodoň, Peter Ševčík</i> Intelligent Mailbox | 54 |

Support for Teaching the Subject Digital Computers

Ondrej Karpiš, Tomáš Bača, Ján Šumský, Michal Kubaščík

Abstract—In this paper, a processor emulator is presented which is used in the teaching of the Digital Computers course. The emulator allows you to create a custom circuit that is controlled by an 8-bit processor via the bus. The processor is emulated by software on the computer and is connected to the circuitry through a special converter. Simulation software has also been created to facilitate the students in creating the circuitry, which allows them to create the circuitry and program without the need for any hardware.

Keywords—processor emulator, simulation tools, teaching support

I. INTRODUCTION

Raising a good programmer is not and never has been an easy task. The rapid development of software technologies in recent years has certainly made programmers' jobs easier. On the other hand, it brings increased demands for orientation in the number of different technologies and supporting tools. These advances have largely been made possible by the development of integrated circuit manufacturing technologies. The speed of a computer's computational core and the size of its operating memory represent a constraint for an increasingly smaller set of problems. In most practical applications, programmers are not constrained by hardware at all. Thus, the world of hardware and software is gradually becoming more distant. Nevertheless, knowledge of the basic principles of digital computer operation belongs to the general education of programmers [1]. That is why at the Faculty of Management science and Informatics of the University of Žilina the subject of Digital Computers has been taught for more than 20 years. Of course, the teaching of this subject is also evolving and adapting to the requirements of the time. The main innovation in the teaching of this subject was the creation of a processor emulator, which is presented in this article.

II. PROCESSOR EMULATOR

A digital computer consists of several main parts: processor, memory, input and output devices [3]. One of the most important tasks in a computer is to provide communication between its parts. It is to deepen the understanding of how the processor communicates with the other parts of the computer using the bus that a simple 8-bit processor emulator was developed. This is not a real processor, it has been designed solely for teaching purposes.

The processor emulator is software-hardware based. The operation of the processor is emulated by the software on the PC. The connection to the hardware bus is made using a special converter which is connected to the PC via USB. A development board is connected to the converter, which contains four 7-segment displays, 16 buttons, one LED and a contact field on which the students make their own circuits. Multiple development boards can be interconnected to implement more complex circuits. The program for the processor must be written in a dedicated assembler. The created program is executed (interpreted) sequentially by a software emulator. The speed of program execution depends on the speed of the computer. In the case of communication of the emulated processor with a converter, the speed is limited by the speed

Ondrej Karpiš, University of Žilina, Slovak Republic (e-mail: ondrej.karpis@fri.uniza.sk)
Tomáš Bača, University of Žilina, Slovak Republic (e-mail: tomas.baca@fri.uniza.sk)
Ján Šumský, University of Žilina, Slovak Republic (e-mail: jan.sumsky@fri.uniza.sk)
Michal Kubaščík, University of Žilina, Slovak Republic (e-mail: michal.kubascik@fri.uniza.sk)

of the USB interface.

A. Processor structure

The proposed processor is of the RISC (Reduced Instruction Set Computers) type and uses the Harvard architecture (i.e. it has separate memory for data and program)[4]. Figure 1 shows its block structure. The processor contains four 8-bit general-purpose registers A, B, C, D. According to the result of mathematical operations, the flag bits of the status register F are set: the Z (Zero) flag is set when the result of an operation is zero and the CY (Carry) flag is set when a register overflow occurs. In addition, the F register also contains the IE flag, which can be used to enable or disable interrupts.

The processor also contains three 16-bit registers:

- PC (Program Counter) - pointer to the following instruction,
- SP (Stack Pointer) - pointer to the top of the stack,
- MP (Memory Pointer) - pointer for indirect addressing of external memory.

Either a constant or a pair of A-B registers can be written to the 16-bit SP and MP registers. The C-D register pair must be used to read from these registers.

The stack size is 64 kB (65536 bytes). The program size is limited to a maximum of 65536 instructions. The processor also contains an internal RAM memory with a size of 256 B. This memory is indirectly addressed by general-purpose registers. It is possible to define a maximum of 256 constants within a program that can be read indirectly using the general-purpose registers.

The width of processor data bus is 8 bits, and the width of the address bus is 16 bits. This corresponds to an address memory space and I/O space with a range of 0-65535. The control bus contains 9 signals, including 5 output signals (Memory Write, Memory Read, Input/Output Write, Input/Output Read, Interrupt Acknowledge) and 4 input signals (Interrupt, Ready, Bus Request, Bus Acknowledge).

B. Interrupts

The processor allows the use of up to 16 interrupts. When an interrupt is requested via the Interrupt signal, if interrupts are enabled, the processor acknowledges receipt of the request with an Interrupt Acknowledge signal. The processor then reads the interrupt handler number (0-15) from the data bus and calls the appropriate interrupt handler. The names of the handlers are int00 - int15. When an interrupt is invoked, the next interrupt is automatically disabled. If there is an instruction in the handler to enable interrupts (usually this instruction is at the end of the handler, but it can be elsewhere), it is also possible to nest interrupts. The number of nested interrupts is limited only by the size of the stack.

An interrupt can be triggered either by the level of the Interrupt signal (when it is at logic level "1") or when the signal changes from "0" to "1". The specific method of triggering an interrupt can be set in the emulation software.

C. Instruction set

The CPU emulator instruction set contains 69 instructions. These instructions can be divided into five basic groups:

- arithmetic and logical instructions: separate instructions are defined if both arguments are in registers (e.g. ADD, SUB, AND, CMP) and if the arguments are a register and a constant (ADI, SBI, ANI, CMI),
- instructions for shifts and rotations (SHL, SCR, RTR ...),
- data transfer instructions (MOV, INN, OUT, PUS, STR, LDR ...),
- branching instructions: in addition to conditional jumps (JZR, JNC, JE, JL ...), conditional

subroutine calls are also available (CNZ, CCY, CNE, CG ...),

- special instructions: enable/disable interrupts; define constant in the program; communicate with the user via the console - character input and output.

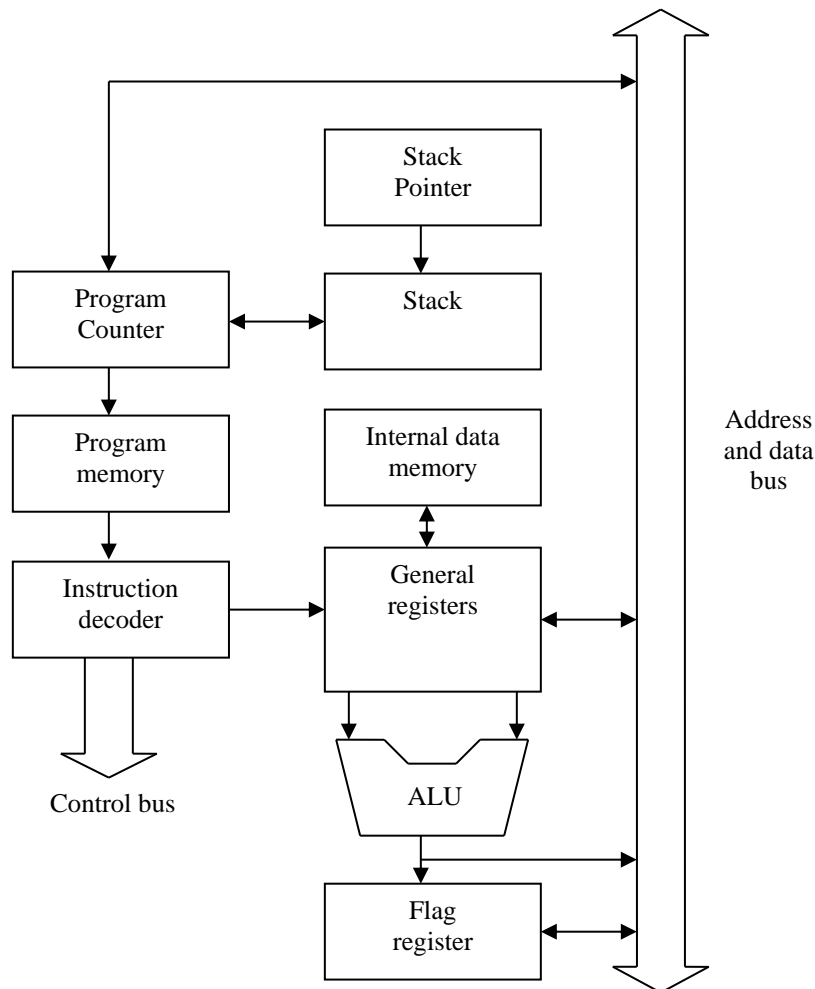


Figure 1 Structure of emulated processor

III. SIMULATION SOFTWARE

In the deployment of the processor emulator in teaching, 20 pieces of converters and 100 pieces of development boards were produced. Due to the high number of students, students had to work in groups. The implementation of the circuits and testing of the developed program was only possible in a dedicated laboratory equipped with converters. The circuits created on the contact field were very sensitive to improper handling. Accidental pulling or breaking of a single wire usually caused a complicated and lengthy search for the fault. This, coupled with limited access to the laboratory, caused problems in completing semester works. For these reasons, a development board simulator was created. Using the simulator, students were able to debug their programs and circuits before implementing them in hardware. They could also work on their semester works in their free time - at home or on campus.

The first version of the software was written in C. This made the simulation of the circuit quite fast. However, the program had limited possibilities in terms of visualization and ease of use. Therefore, a new version of the software was created, this time in Java. This made it possible to use the program not only in Windows operating system but also in Linux and iOS.

The new software also brought a more graphically appealing interface, more data display formats, graphical differentiation of individual parts of the program (instructions of different types, constants, labels, comments), the possibility of using more parts of the development system (contact fields, displays, keyboards, LEDs), the possibility of visualizing the current state of the circuits (logic levels of inputs and outputs, content of the registers or memory). The simulation software also indicates some errors that can be caused by improper connection (e.g. short circuit).

The simulation software uses two separate windows - one showing the processor parts (registers, stack, internal memory) together with the user program, and the second window showing the circuit simulator. Both windows are shown in Figure 2.

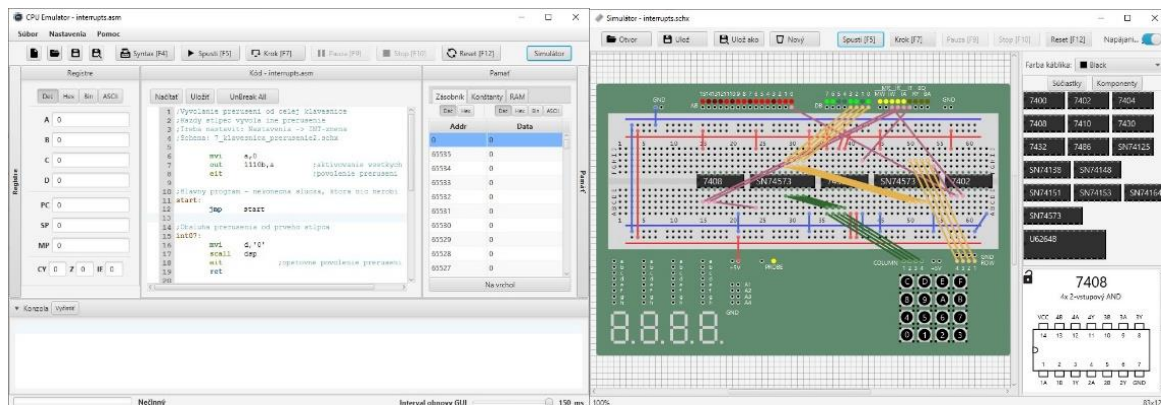


Figure 2 Processor emulator (on the left) and circuit simulator

Of course, the created simulator has some shortcomings. The main drawback is the imperfect simulation of the behavior of the logic circuits involved. In most cases the simulation is sufficiently faithful, but in special cases the simulator behavior is different from the behavior of the real circuitry. The second drawback is the limited number of types of integrated circuits that can be used in the circuitry. Also note that the speed of the simulation is dependent on the speed of the computer. The loss of physical contact with the hardware can also be considered as a disadvantage.

Despite the above disadvantages, the use of a simulator has undeniable positives. Mainly, it simplifies and facilitates the work of students in creating the circuitry and they can spend more time on creating the program or create more complex circuitry. The simulator also eliminates the need for regular repairing of malfunctioning or damaged hardware parts - converters, integrated circuits and development boards. For these reasons, the hardware processor emulator has gradually been replaced by the simulator.

IV. CONCLUSION

Based on our experience, we can conclude that the use of a processor emulator in the teaching of the Digital Computers course helps students to understand the principles of operation of digital computers. The acquired knowledge is much more durable due to the practical experience. Although most of the students who take this course are software developers, every year there are a few students who are intrigued by the possibility of creating their own circuitry and they produce very original semester works. The interest of these students is the reason why it makes sense to continue to develop similar learning support tools.

REFERENCES

- [1] Hassan, M. K., & Rana, M. M. "An Overview of Embedded Systems and Applications in Education," *IEEE Transactions on Education*, vol. 58, no. 3, pp. 123-134, 2015.
- [2] S. S. Anwar, S. A. Usmani, and M. R. K. Raju, "A review on embedded systems: Opportunities and challenges in future," *IEEE Transactions on Industrial Electronics*, vol. 55, no. 3, pp. 1005-1017, 2008.
- [3] W. Stallings, *Computer Organization and Architecture: Designing for Performance*, 10th ed., Pearson, 2016.
- [4] M. Moradi, "A Survey on Modern Microprocessor Architectures," *IEEE Access*, vol. 9, pp. 53323-53340, 2021.

Measuring Kinetic Energy from Tree Movements Induced by Wind

Tomáš Bača, Ján Šumský, Michal Kubaščík, Peter Šarařín

Abstract—The movement of trees as a response to wind presents an underexploited renewable energy source. Wind as a renewable energy source is highly unpredictable. This research focuses on creating wireless sensors and data acquisition systems that are used to measure the dynamical properties of tree movements, such as amplitude and frequency. The sensors are based on the use of the IMU – Inertial Measurement Unit sensor and utilizes the newest MCUs from Espressif.

Keywords—Kinetic energy, Accelerometer, Gyroscope, Microcontroller, Bluetooth, WSN

I. INTRODUCTION

The quest for renewable energy sources is a global challenge. Traditional energy sources, such as fossil fuels, contribute significantly to environmental degradation and climate change. Renewable energy sources, while promising, often face challenges related to consistency and environmental impact. Wind energy, in particular, is abundant but highly unpredictable. This research addresses the potential of harnessing energy from the natural movements of trees, such as tree sway and leaf vibration, induced by wind. By developing wireless sensors and data acquisition systems to measure these movements.

A. Trees as a source of energy

The importance of finding sustainable energy sources cannot be overstated, given the environmental impact of conventional energy sources.

Energy harvesting from tree movements offers a unique opportunity to generate power in an eco-friendly manner.

By leveraging the natural sway and vibration of trees, we can develop a reliable energy source that mitigates the need for batteries in forest environments. Traditional batteries pose a risk of leaking chemicals, which can be detrimental to the ecosystem.

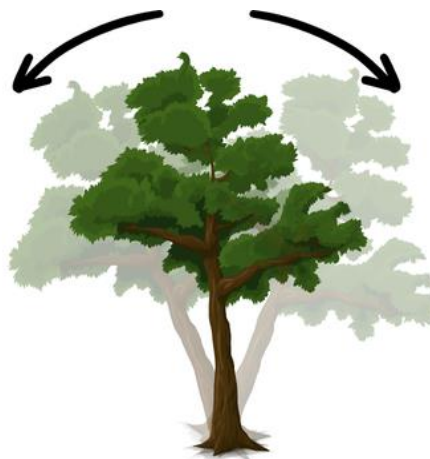


Figure 1-Tree sway

Tomáš Bača, University of Žilina, Slovak Republic (e-mail: tomas.baca@fri.uniza.sk)
Ján Šumský, University of Žilina, Slovak Republic (e-mail: jan.sumsky@fri.uniza.sk)
Michal Kubaščík, University of Žilina, Slovak Republic (e-mail: michal.kubascik@fri.uniza.sk)
Peter Šarařín, University of Žilina, Slovak Republic (e-mail: peter.sarafin@fri.uniza.sk)

B. *Defining the sway*

Tree sway refers to the back-and-forth movement of trees caused by wind. This natural phenomenon occurs when wind forces act on the tree, causing the trunk to sway and the branches to oscillate. The dynamics of tree sway depend on several factors, including tree height, trunk flexibility, branch structure, and wind speed. Understanding tree sway is crucial for developing systems that can harness this kinetic energy effectively. Measuring the amplitude and frequency of tree sway provides insights into the energy potential of this natural movement. [1][2]

C. *Defining oscillation*

Oscillation refers to the repetitive back-and-forth movement around a central point or equilibrium position. In the context of tree sway, oscillation describes the periodic motion of tree branches and trunks as they respond to wind forces. This movement can be characterized by two main properties: amplitude and frequency.

Amplitude: This is the maximum extent of the oscillation, measured from the equilibrium position to the peak of the movement. For trees, the amplitude of sway indicates how far the tree moves from its resting position when subjected to wind.

Frequency: This is the number of oscillations that occur in a given time period, typically measured in cycles per second (Hertz). In trees, the frequency of sway is influenced by factors such as the tree's height, mass distribution, and flexibility.

Understanding oscillation is critical for modeling the dynamic behavior of trees under wind load and for assessing the potential of harvesting kinetic energy from tree movements. By analyzing the amplitude and frequency of oscillation, we can gain insights into the energy transfer processes and the mechanical properties of trees, which are essential for designing efficient energy harvesting systems. [3]

D. *Measuring tree movements*

We begin by collecting data on the tree's movements. This involves deploying a series of wireless sensors that capture the dynamical properties of tree sway, such as amplitude and frequency. These sensors, including accelerometers and gyroscopes, are strategically placed at different heights and positions on the tree to ensure comprehensive data collection. The accelerometers measure the linear acceleration in three-dimensional space, providing insights into both horizontal and vertical movements, while the gyroscopes measure the rotational motion.

The data is then transmitted for analysis and modeling.

II. WAYS TO MEASURE TREE MOVEMENTS

There are several ways to measure the movements of trees, some well-known and others less so. Let's explore some of these methods.

A. *IMUs*

Inertial Measurement Units (IMUs) combine multiple sensors, including gyroscopes and accelerometers, to provide comprehensive data on tree sway and vibration. Tilt sensors, also known as inclinometers, can measure the angle of tilt or inclination of the tree trunk from a vertical position. The gyroscope within the IMU can measure tilt and rotational motion, while the accelerometer measures linear acceleration, capturing the dynamic properties of tree movements.

B. *Accelerometers*

Accelerometers measure the acceleration of the tree trunk in different directions. By setting

up an accelerometer directly on the tree, the device can directly measure the trunk's sway. This data is crucial for analyzing how different parts of the tree move in response to wind forces, capturing both horizontal and vertical movements. [4][5]

C. Strain Gauges

Strain gauges measure the deformation, or strain, of the tree, allowing monitoring of how the tree's shape changes in response to wind and other forces. This method is useful for understanding the stress distribution within the tree structure.

D. Magnetic Sensors

Magnetic sensors can measure the displacement of tree branches by capturing small movements over a limited distance. However, installation can be challenging due to the need for precise alignment and calibration.

E. Optical Measurement Techniques

Lasers and other optical measurement techniques can be used to measure tree movements by detecting changes in distance or position with high precision. These methods are typically more expensive but offer high accuracy.

Each measurement method offers unique benefits and challenges, and the choice of sensor depends on the specific requirements of the study, including the type of data needed, the environment, and the available budget.

F. Working with IMUs

To effectively measure the movement of trees, we employ IMUs, which integrate accelerometers and gyroscopes. IMUs provide a detailed analysis of both linear acceleration and rotational motion.

1) Accelerometers

Accelerometers measure the acceleration of an object in one or more axes. When attached to a tree, they can detect changes in velocity as the tree moves back and forth due to wind forces. Inside an accelerometer, a small mass is suspended by springs. When the device accelerates, the mass shifts, causing a change in the electrical signal proportional to the acceleration. This signal helps determine the direction and magnitude of the tree's movement.

2) Gyroscopes

Gyroscopes measure the rate of rotation around the axes, capturing the tilt and rotational motion of the tree trunk and branches. This is essential for understanding the twisting and turning movements that occur in response to wind.

G. Types of Data Harvested

Accelerometers provide several types of data essential for analyzing tree movements:

1) Linear Acceleration

This measures the rate of change of velocity in three-dimensional space (X, Y, and Z axes). For trees, this data helps in understanding how different parts of the tree move in response to wind forces, capturing both horizontal and vertical movements.

2) Amplitude of movement

By integrating the acceleration data over time, we can determine the displacement of the tree. The amplitude gives us the maximum extent of the tree's sway, which is crucial for estimating the energy that can be harvested.

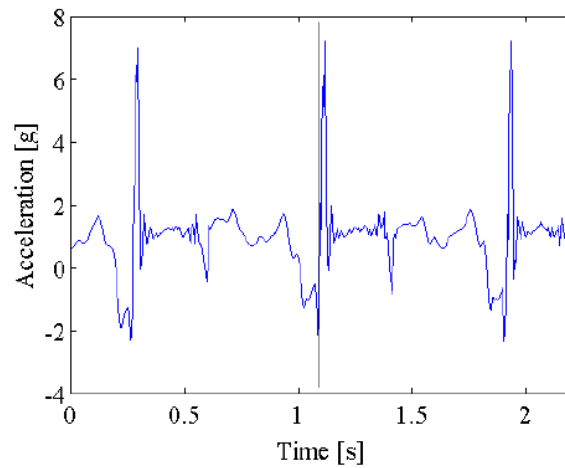


Figure 2- Accelerometer data example [6]

H. Frequency of sway

The accelerometer data can be analyzed using Fourier transforms to determine the dominant frequencies of the tree's movement. This information helps in identifying the natural oscillation patterns of the tree, which can be correlated with wind speed and direction.

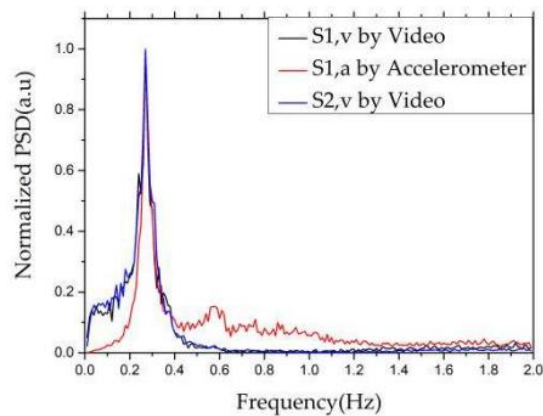


Figure 3- Frequency Spectrum example [7]

I. Vibration analysis

Accelerometers are sensitive enough to detect minute vibrations. This capability allows us to study not only the large-scale movements but also the small vibrations that can provide insights into the structural health of the tree and its response to varying wind conditions.

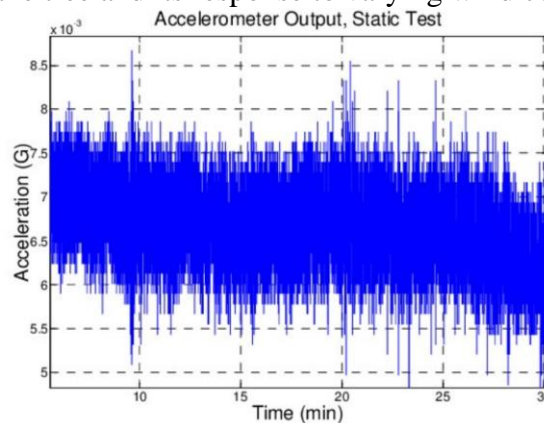


Figure 4- Vibration graph [8]

We are planning to also use an anemometer in order to know the wind speed. This will allow us to correlate the wind speed with the measured sway of the trees. By comparing this data with the accelerometer readings, we can establish a detailed understanding of how different wind speeds and gusts influence tree movements. Understanding the relationship between wind speed and tree sway will also help in optimizing the placement of sensors and enhancing the overall efficiency of the energy harvesting system.

III. METHODOLOGY

This section details the methodology used to measure the dynamic properties of tree movements. We utilize a Wireless Sensor Network (WSN) consisting of sensors, microcontrollers, and data storage systems, each playing a specific role in capturing and processing the data. The components involved include Measurement Nodes (M-Nodes), Anemometer Nodes (A-Nodes), Sleepers, Communication Nodes (COM-Nodes), Wi-Fi Nodes (WIFI-Nodes), and a Communication Module (COM-MODULE). [9]-[12]

A. Types of Sensors

We use a variety of sensors to capture the necessary data:



Figure 5- Xiao seeed nRF52840 [13]

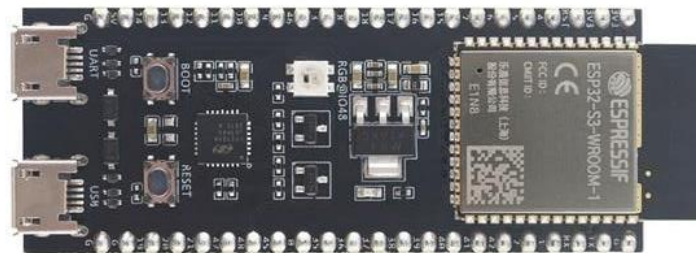


Figure 6- ESP32-S3 [14]

1) M-Nodes

These are nRF sensors equipped with accelerometers. We use four such sensors, each attached to different parts of the tree to measure various aspects of its movement. The nRF sensors transmit their data wirelessly to the COM-node. The accelerometers measure linear acceleration in three axes, providing comprehensive data on the tree's sway and vibration.

2) A-Nodes

An anemometer is used to measure wind speed, providing essential data for understanding the external forces acting on the tree. The anemometer sends this data to the COM-node as well.



Figure 7- Anemometer with a fin [15]

3) Sleepers

These are nRF modules placed on the branch stump, equipped with batteries. They enter a sleep mode to conserve energy and periodically wake to measure the voltage and transmit this data. This helps in monitoring the power supply and ensuring the longevity of the system.

4) COM-Nodes

The ESP32-S3 microcontroller serves as the Communication Node, receiving data from the nRF sensors via Bluetooth Low Energy (BT LE). The COM-Node processes the data before sending it to the Wi-Fi Node.

5) WIFI-Nodes

The other ESP32-S3 microcontroller acts as the Wi-Fi Node, responsible for storing the processed data on an SD card. This ensures that we have a robust and reliable record of the tree's movements and the corresponding wind conditions.

6) COM-Module

The COM-Module refers to both ESP32-S3 microcontrollers working together to collect, process, and store the data from the sensors.

B. Sensor Placement

The placement of sensors is crucial for accurately capturing the dynamic properties of tree movements. By strategically positioning sensors, we can ensure that the data collected is both accurate and representative of the tree's natural movements.

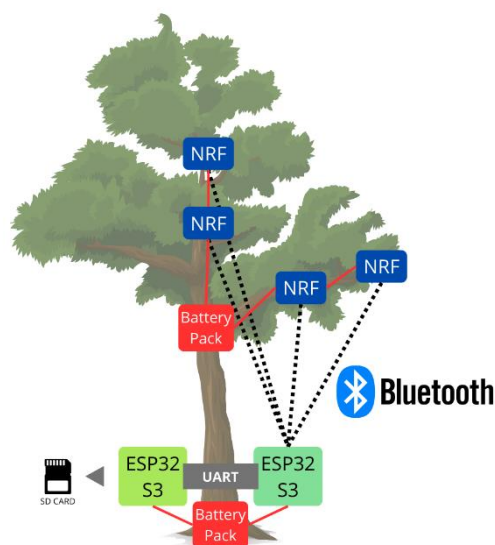


Figure 8- Sensor placement

1)M-Node Placement

M-Nodes are placed at various heights and locations on the tree to capture comprehensive movement data. By positioning these sensors on the trunk and major branches, we can measure the tree's sway and vibration across different parts of the tree. This helps in understanding the distribution of movement and the impact of wind forces.

2)A-Node Placement

The A-Node, or anemometer, is positioned in an open area near the tree to measure wind speed without obstruction. Accurate wind speed data is essential for correlating tree movements with external wind forces.

3)Sleeper Placement

Sleepers are placed on the branch stump to monitor the power supply. These nodes wake periodically to measure voltage and ensure that the sensors are functioning correctly and have sufficient power.

4)COM-Node and WIFI-Node Placement

The COM-Node (ESP32-S3) is positioned within the range of the nRF sensors to receive data via BT LE efficiently. The WIFI-Node (ESP32-S3) is located nearby to facilitate data storage on an SD card, ensuring minimal data loss and reliable long-term storage.

C. Data Transmission and Storage

The collected data from the M-Nodes and A-Nodes is transmitted to COM-Node (ESP32-S3) via BT LE. The COM-Node further processes the data and transmits it to the WIFI-Node (ESP32-S3), where it is stored on an SD card for offline analysis. This multi-stage data transmission process ensures data integrity and reliability.

D. Data Analysis

The data stored on the SD card is analyzed to understand the dynamic properties of tree movements. Key parameters such as linear acceleration, amplitude of movement, frequency of sway, and vibration are extracted. Fourier transforms are applied to determine the dominant frequencies of the tree's movement, providing insights into natural oscillation patterns. The relationship between wind speed and tree sway is also analyzed to optimize the placement of sensors and enhance the overall efficiency of the energy harvesting system.

E. Energy consumption

The energy consumption of the WSN could be decreased by putting the M-Nodes into deep sleep and waking them up only when the A-Nodes measure winds with speed above a certain threshold. This is known as event-driven measurement. The other way how to save energy could be the use of compressed sensing which however has its own problems. [16]-[18]

Another way to decrease the power consumption of the M-nodes is by using low power wireless communication technologies. We are currently using the Bluetooth Low Energy for communication between the M-nodes and COM-node. But other alternatives for low power wireless communication could be LPWAN, Sigfox or LoRaWan. [19][20]

IV. POSSIBILITIES AND RECOMMENDATIONS FOR MEASUREMENT ON REAL TREES

Implementing measurement systems on real trees involves several considerations and recommendations to ensure accurate and reliable data collection. [21]

Sensor placement: It is crucial to strategically place the sensors at various heights and positions on the tree to capture a comprehensive range of movement. Sensors should be secured firmly to prevent detachment due to high winds or other environmental factors.

Power supply: Powering the sensors in a forest environment can be challenging. Options include energy harvesting from tree movements themselves, or long-lasting batteries. Each

method has its own set of advantages and limitations that need to be evaluated based on the specific site conditions. The usage of sleep function on the nRF can greatly improve the span of life of the battery, which means that it does not require as much energy as a full-time working device. [22]

Environmental protection: The sensors and associated electronics must be protected from harsh weather conditions, including rain, snow, and extreme temperatures. Waterproof enclosures and robust materials are essential for the longevity and reliability of the measurement system.

Calibration and validation: Regular calibration of sensors is necessary to ensure data accuracy. Additionally, it is recommended to validate the sensor data with other measurement methods or reference devices to confirm the reliability of the readings.

V. FUTURE RESEARCH DIRECTION

The preliminary phase of next step involves selecting the appropriate tree for sensor placement and deciding the mode of data communication. Initial experiments will focus on choosing an optimal tree based on factors such as size, location, and accessibility. Data collected from the sensors can be stored either on an SD card for offline analysis or transmitted via Wi-Fi for real-time monitoring.

Early analyses of the collected data will help in understanding the dynamics of tree sway and the effectiveness of different sensors in capturing this movement. The insights gained from these initial results will guide further refinement of the sensor setup and data collection methods.

Future research will extend beyond the deployment of sensors to include the development of energy harvesting systems that can capture and store the energy generated from tree sway. While this paper focuses on the implementation and analysis of tree sway sensors, subsequent studies will explore the integration of energy harvesting technologies to convert the mechanical energy of tree movements into usable electrical energy. This comprehensive approach aims to establish a sustainable method for harnessing renewable energy from natural sources like tree sway.

VI. CONCLUSION

In conclusion, the movement of trees in response to wind represents a new and underexploited source of renewable energy. This research demonstrates the feasibility of using wireless sensors and data acquisition systems to measure and analyze the dynamic properties of tree movements. By employing forecasting algorithms, we can predict the availability of this energy source based on weather conditions. The successful implementation of this system in real-world conditions requires careful consideration of sensor placement, power supply, data transmission, environmental protection, and regular calibration.

Future work will focus on refining these systems and the implementation of the project through initial tests. These tests will be conducted on several trees to evaluate the performance and reliability of the sensors and data acquisition systems under different conditions. Additionally, further development of forecasting algorithms will be undertaken to improve the accuracy and predictability of energy harvesting potential.

Ultimately, the goal is to develop a robust and scalable solution that can be deployed in forests worldwide, contributing to the global effort to harness renewable energy sources and promote sustainable development.

The energy storage subsystem in this solution will use supercapacitors and maximum power point tracking (MPPT) algorithms to achieve small energy losses during energy storage and a sufficient amount of recharge cycles of the energy storage subsystem.[23]

REFERENCES

- [1] A. Wang, X. Yang, and D. Xin, "The tracking and frequency measurement of the sway of leafless deciduous trees by adaptive tracking window based on MOSSE," *Forests*, vol. 13, no. 1, 2022. [Online]. Available: <https://www.mdpi.com/1999-4907/13/1/81>
- [2] T. Jackson et al., "The motion of trees in the wind: A data synthesis," *Biogeosciences*, vol. 18, pp. 4059–4072, Jul. 2021. [Online]. Available: https://www.researchgate.net/publication/353016186_The_motion_of_trees_in_the_wind_A_data_synthesis
- [3] F. Zanotto, L. Marchi, and S. Grigolato, "Preliminary results of a novel approach to assess the fundamental sway frequency of trees," in *2022 IEEE Workshop on Metrology for Agriculture and Forestry (MetroAgriFor)*, 2022, pp. 150–154. [Online]. Available: <https://ieeexplore.ieee.org/document/9965061>
- [4] D. Jaeger et al., "From flowering to foliage: Accelerometers track tree sway to provide high-resolution insights into tree phenology," *Agricultural and Forest Meteorology*, vol. 318, p. 108900, May 2022. [Online]. Available: <https://www.sciencedirect.com/science/article/pii/S0168192322000934>
- [5] T. van Emmerik et al., "Measuring tree properties and responses using low-cost accelerometers," *Sensors*, vol. 17, no. 5, May 2017. [Online]. Available: <https://www.mdpi.com/1424-8220/17/5/1098>
- [6] B. Eskofier, E. Musho, and H. Schlarb, "Pattern classification of foot strike type using body-worn accelerometers," May 2013. [Online]. Available: https://www.researchgate.net/publication/261451344_Pattern_classification_of_foot_strike_type_using_body_worn_accelerometers
- [7] M. Chen et al., "A temperature insensitive strain sensor based on SMF-FMF-NCF-FMF-SMF with core-offset fusion," Dec. 2023. [Online]. Available: https://www.researchgate.net/publication/376310468_A_temperature_insensitive_strain_sensor_based_on_SMF-FMF-NCF-FMF-SMF_with_core-offset_fusion
- [8] J. Collin and G. Lachapelle, "MEMS-IMU for personal positioning in a vehicle—a gyro-free approach," Jan. 2002. [Online]. Available: https://www.researchgate.net/publication/255668676_MEMS-IMU_for_personal_positioning_in_a_vehicle-A_gyro-free_approach
- [9] O. Karpis et al., "Compressed sensing—a way to spare energy in WSN for UAV," *FAC PapersOnline*, vol. 55, no. 4, SI, pp. 170–176, 2022. [Online]. Available: <https://www.sciencedirect.com/science/article/pii/S2405896322003433>
- [10] P. Sevcik, S. Zak, and M. Hodon, "Wireless sensor network for smart power metering," *Concurrency and Computation: Practice and Experience*, vol. 29, no. 23, SI, Dec. 2017. [Online]. Available: <https://onlinelibrary.wiley.com/doi/10.1002/cpe.4247?msocid=1dd4a3b972136d971c72b01f73ba6c76>
- [11] M. Hodon et al., "Application of WSN for smart power metering to avoid cheating on electric power consumption at places with shared power," in *Proceedings of the 2015 Federated Conference on Computer Science and Information Systems*, 2015, pp. 1215–1221. [Online]. Available: <https://ieeexplore.ieee.org/document/7321583>
- [12] V. Olesnanikova et al., "Water level monitoring based on the acoustic signal using the neural network," 2016, pp. 203–206. [Online]. Available: <https://www.scopus.com/record/display.uri?eid=2-s2.0-84988805249&origin=cto>
- [13] Farnell, "Seed studio 102010448." [Online]. Available: <https://sk.farnell.com/seed-studio/102010448/xiao-board-arm-arduino-board/dp/4060351>
- [14] Makerguides, "Choosing the best Arduino board: A comparison of 8 options." [Online]. Available: <https://www.makerguides.com/choosing-the-best-arduino-board/>
- [15] Amazon, "Wind speed sensor three cups anemometer wind speed and direction meteorological transmitter measuring instrument smart weather station (color: 1, size: 21)." [Online]. Available: <https://www.amazon.sg/Anemometer-Direction-Meteorological-Transmitter-Instrument/dp/B0BD71434J>
- [16] M. Kochlan and M. Hodon, "Impact of external phenomena in compressed sensing methods for wireless sensor networks," in *Proceedings of the 2017 Federated Conference on Computer Science and Information Systems (FedCSIS)*, 2017. [Online]. Available: <https://ieeexplore.ieee.org/document/8104651>
- [17] M. Hodon et al., "Maximizing performance of low-power WSN node on the basis of event-driven-programming approach: Minimization of operational energy costs of WSN node control unit," in

- 2015 *IEEE Symposium on Computers and Communication (ISCC)*, Feb. 2016, pp. 204–209. [Online]. Available: <https://ieeexplore.ieee.org/document/7405517>
- [18] P. Sevcik et al., "Maximizing performance of low-power WSN node on the basis of event-driven-programming approach: Minimization of operational energy costs of WSN node control unit," in *2015 IEEE Symposium on Computers and Communication (ISCC)*, 2015, pp. 204–209. [Online]. Available: <https://ieeexplore.ieee.org/document/7405517>
- [19] M. Chochul and P. Sevcik, "A survey of low power wide area network technologies," in *2020 18th International Conference on Emerging eLearning Technologies and Applications (ICETA)*, 2020, pp. 69–73. [Online]. Available: <https://ieeexplore.ieee.org/document/9379213>
- [20] O. Karpis, "Sensor for vehicles classification," 2012, pp. 785–789. [Online]. Available: <https://www.scopus.com/record/display.uri?eid=2-s2.0-84892890755&origin=cto>
- [21] S. McGarry and C. Knight, "Development and successful application of a tree movement energy harvesting device to power a wireless sensor node," *Sensors*, vol. 12, no. 9, pp. 12110–12125, Sep. 2012. [Online]. Available: <https://www.mdpi.com/1424-8220/12/9/12110>
- [22] C. Knight, J. Davidson, and S. Behrens, "Energy options for wireless sensor nodes," *Sensors*, vol. 8, no. 12, pp. 8037–8066, Dec. 2008. [Online]. Available: <https://www.mdpi.com/1424-8220/8/12/8037>
- [23] M. Kochlan et al., "Performance of open voltage control algorithm for sensor node power management unit," in *2016 International Conference on Information and Digital Technologies (IDT)*, 2016, pp. 138–143. [Online]. Available: <https://ieeexplore.ieee.org/document/7557163>

Universal System for Indoor Location

Richard Boťanský, Michal Hodoň, Lukáš Čechovič, Peter Ševčík

Abstract— The aim of this paper was to make an application which can provide indoor localization. The application is made from three components: iBeacons, Raspberry Pi and web server. Result consists of two web applications. First web application runs on Raspberry Pi, which communicates with iBeacons through Bluetooth. Second web application runs on web server, which communicates with Raspberry Pi.

Keywords— indoor localization, communication through Bluetooth, iBeacon, Raspberry Pi, Flask application, web application.

I. INTRODUCTION

Indoor localization has emerged as a critical technology in various domains, including logistics, smart buildings, healthcare, and retail. Unlike outdoor localization systems such as GPS, which rely on satellite signals, indoor environments present unique challenges, including signal attenuation, multipath interference, and the presence of physical obstacles such as walls and furniture. These limitations necessitate the adoption of alternative localization technologies specifically designed for indoor use [1], [2]. Bluetooth Low Energy (BLE) technology, introduced with Bluetooth 4.0, has gained significant attention as a promising solution for indoor localization due to its low power consumption, cost-effectiveness, and compatibility with a wide range of devices [3]. Among BLE-based solutions, iBeacons—developed by Apple Inc.—stand out for their simplicity and widespread adoption. iBeacons transmit unique identifiers that can be processed by receiving devices, enabling proximity detection and relative localization [4], [5]. In this study, we propose a system that leverages iBeacon technology, Raspberry Pi devices, and a web server to create an efficient and scalable indoor localization framework. The Raspberry Pi acts as a receiver, capturing BLE signals from iBeacons, while the web server processes and visualizes the data in real-time. By addressing the limitations of existing systems and integrating robust hardware and software components, this system aims to offer a reliable solution for tracking objects and personnel in indoor spaces. The motivation for this work stems from the increasing demand for precise indoor localization systems in industries where real-time tracking can enhance operational efficiency and user experience. From tracking assets in warehouses to enabling navigation in large public buildings, the potential applications of indoor localization are vast and diverse [6], [7]. This paper details the design, development, and evaluation of the proposed system. It discusses the selection of hardware and software components, the methodology for signal processing and communication, and the results obtained from experimental testing. The integration of Internet of Things (IoT) devices into daily life offers significant opportunities for reducing energy wastage and enhancing sustainability. Among these innovations, smart sockets stand out for their ability to provide real-time insights and control over energy consumption. This paper explores the conceptualization, design, and practical implementation of a smart socket tailored to address the growing demand for smarter, more energy-efficient homes.

II. INTEGRATION

The methodology for the indoor localization system was developed to integrate hardware, software, and calibration processes into a cohesive and reliable solution. The system utilized

Richard Boťanský, University of Zilina, Zilina, Slovakia (e-mail: botansky@stud.uniza.s)
Michal Hodoň, University of Zilina, Zilina, Slovakia (e-mail: michal.hodon@fri.uniza.sk)
Lukáš Čechovič, University of Zilina, Zilina, Slovakia (e-mail: lukas.cechovic@fri.uniza.sk)
Peter Ševčík, University of Zilina, Zilina, Slovakia (e-mail: peter.sevcik@fri.uniza.sk)

iBeacons as BLE transmitters, broadcasting unique identifiers and RSSI values. These transmitters were strategically positioned to ensure coverage across the designated indoor space. Signals from the iBeacons were received by Raspberry Pi devices configured with Bluetooth adapters and programmed using Python scripts. The Raspberry Pi devices processed the received signals and estimated distances using calibrated RSSI-distance models. Signal processing involved filtering techniques to minimize noise and mitigate the effects of multipath interference, ensuring the accuracy of distance estimations. The Raspberry Pi devices also hosted lightweight web servers built using Flask, enabling data communication with a central server over a local network. Standard TCP/IP protocols facilitated this communication, ensuring seamless data transfer. The central server was developed using CakePHP for backend processing and Vue.js for frontend visualization. It aggregated data from multiple Raspberry Pi devices and maintained a MySQL database for storing real-time and historical localization data. The server used this data to compute object locations through algorithms such as trilateration or centroid-based methods. A user-friendly web-based dashboard provided access to localization data, offering features such as movement tracking, zone-based analysis, and visual representations of object positions. The calibration process was a fundamental part of the methodology, aimed at establishing reliable correlations between RSSI values and physical distances. Signal strength data was collected at defined distances, and filtering techniques were applied to refine this data by reducing noise and environmental interference. Calibration data was iteratively refined to ensure consistency and accuracy, enabling the system to perform effectively across varying indoor conditions. The system architecture comprised three layers. The sensing layer collected BLE signals from iBeacons, the processing layer handled signal refinement and data communication via the Raspberry Pi devices, and the visualization layer presented the processed data through the web dashboard. This structured approach allowed for the efficient integration and management of system components, ensuring that the system met the operational requirements of indoor localization in diverse application areas.

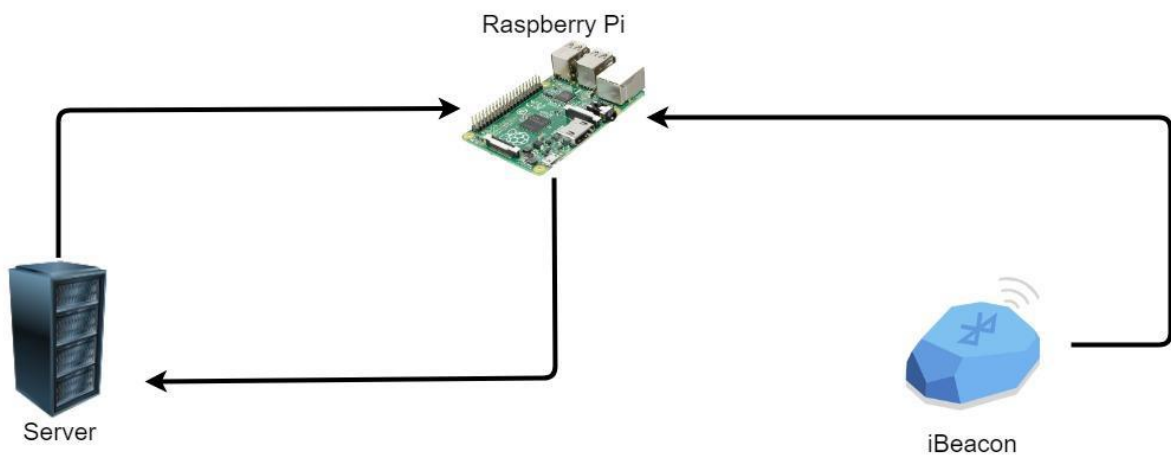


Fig. 1 System block schematic

| calibration_beacons | |
|---------------------|-------|
| PK | id |
| | name |
| | value |

| nearby_beacons | |
|----------------|------|
| PK | id |
| | name |
| | type |
| | time |

| last_updates | |
|--------------|------------|
| PK | id |
| | time |
| | name_table |
| | value |

Fig. 2 RPi Database

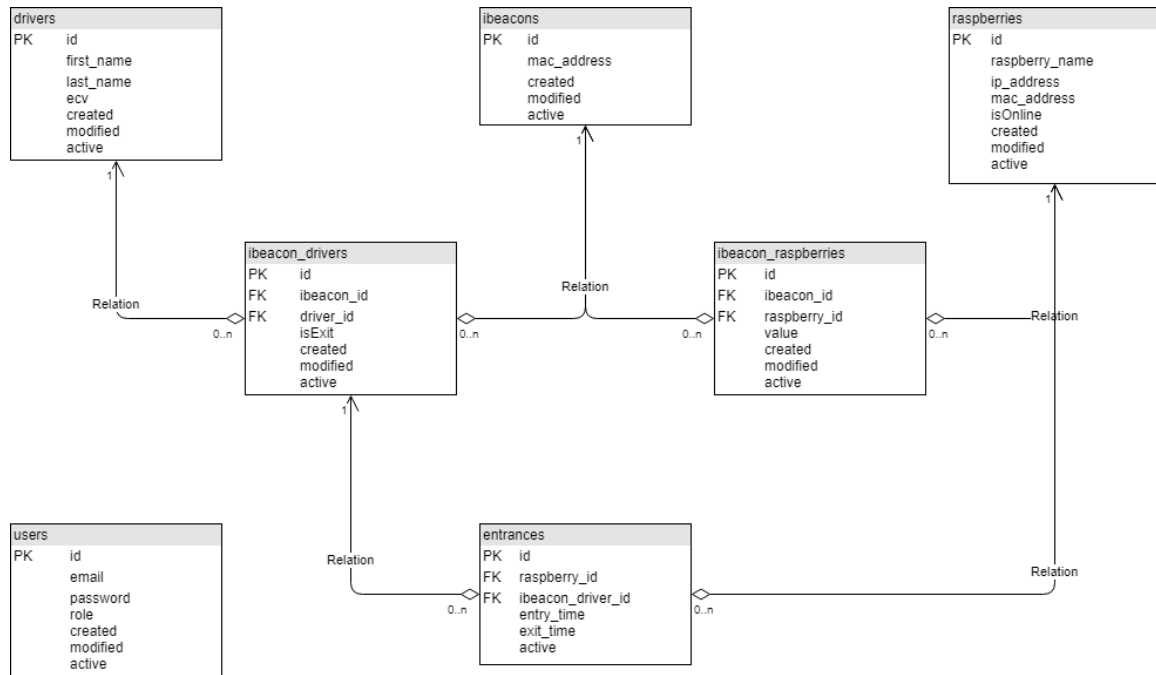


Fig. 3 Web application database schematic

III. CONCLUSION

The developed system was tested in a controlled environment with multiple iBeacons placed at known locations. Raspberry Pi devices accurately captured BLE signals and transmitted data to the web server. Calibration routines improved the precision of distance measurements. The web interface successfully displayed real-time localization data, showcasing the system's potential in practical applications. The proposed system demonstrated a high degree of accuracy in indoor localization tasks. However, signal attenuation due to physical obstructions such as walls and human bodies posed challenges in certain scenarios. The choice of iBeacons and BLE technology proved cost-effective and scalable. Future work could focus on integrating machine learning algorithms to enhance accuracy and exploring additional applications in healthcare and retail. This study successfully implemented an indoor localization system using iBeacon technology, Raspberry Pi devices, and a web server. The system offers a cost-effective and scalable solution for indoor localization, with potential applications across various industries. Future enhancements could include optimizing signal processing algorithms and expanding the system's functionality.

REFERENCES

- [1] J. Hightower and G. Borriello, "Location systems for ubiquitous computing," *IEEE Computer*, vol. 34, no. 8, pp. 57-66, 2001.
- [2] P. Spachos and D. Hatzinakos, "BLE beacons in the smart city: Applications, challenges, and research opportunities," *IEEE Communications Magazine*, vol. 55, no. 11, pp. 76-81, 2017.
- [3] Bluetooth SIG, "Bluetooth Low Energy Overview," 2020. [Online]. Available: <https://www.bluetooth.com/learn-about-bluetooth/bluetooth-technology/bluetooth-low-energy/>. [Accessed: Dec. 6, 2024].
- [4] Apple Inc., "iBeacon for Developers," 2013. [Online]. Available: <https://developer.apple.com/ibeacon/>. [Accessed: Dec. 6, 2024].
- [5] T. Li, Y. Zhang, and R. Zhang, "A survey on mobile phone sensing, positioning, and tracking," *IEEE Communications Surveys & Tutorials*, vol. 17, no. 2, pp. 597-617, 2015.
- [6] J. Krumm, "A survey of computational location privacy," *Personal and Ubiquitous Computing*, vol. 13, pp. 391-399, 2009.
- [7] M. Z. Win et al., "Network localization and navigation via cooperation," *IEEE Communications Magazine*, vol. 49, no. 5, pp. 56-62, 2011.

Wireless Voting System

Adrián Hložný, Michal Hodoň, Lukáš Formanek

Abstract— This paper presents the development and implementation of a wireless voting system utilizing ESP32 technology. The system comprises a voting device powered by a Li-Pol battery and a collector device connected via the ESP-NOW protocol. The voting device processes user inputs for multiple-choice questions and transmits responses wirelessly to the collector device. Collected data is visualized as a bar graph on a web page managed by the collector device. The system aims to provide an efficient, cost-effective, and environmentally friendly alternative to traditional voting methods. Results from prototype testing demonstrate the system's functionality and highlight its potential applications in educational and organizational settings.

Keywords— ESP32, ESP-NOW, Li-Pol battery, micro-USB, web page.

I. INTRODUCTION

Voting systems play a critical role in decision-making processes across various domains, including legislative assemblies, corporate environments, educational institutions, and public referendums. Traditional voting methods, such as paper-based ballots or manual tallying, are often inefficient, prone to errors, and environmentally unsustainable due to significant resource consumption. As the demand for more efficient and reliable systems grows, technological advancements in electronics and wireless communication offer promising solutions to modernize these processes [1], [2]. The integration of Internet of Things (IoT) technologies into voting systems has the potential to address many of the limitations of traditional approaches. IoT-enabled voting systems can provide real-time communication, secure data processing, and enhanced user convenience. Among the various IoT platforms available, the ESP32 microcontroller has emerged as a cost-effective and versatile solution for wireless applications [3], [4]. Its ability to support multiple communication protocols, such as WiFi and ESP-NOW, makes it particularly suitable for building scalable and efficient systems [5]. This paper focuses on the development of a wireless voting system utilizing ESP32 technology and the ESP-NOW protocol. ESP-NOW, a proprietary communication protocol by Espressif Systems, enables low-latency and reliable peer-to-peer data transmission without requiring an active WiFi network. This feature allows the system to operate independently of external network infrastructure, increasing its flexibility and reducing setup complexity [6] [7]. The system's primary components include a voting device that captures user inputs and a collector device that aggregates and visualizes the results. The design emphasizes ease of use, low power consumption, and environmental sustainability, making it suitable for a wide range of applications. In addition to addressing operational inefficiencies, this study aims to explore the feasibility of implementing a compact, portable, and user-friendly voting system for educational and organizational settings. Such systems could enhance participation rates, streamline decision-making processes, and provide real-time feedback to users. By leveraging modern microcontroller technologies and efficient communication protocols, the proposed system seeks to deliver a reliable and scalable solution that aligns with the needs of contemporary users. This paper outlines the methodology for designing the system, discusses the results of performance evaluations, and highlights its potential applications and limitations. The proposed solution contributes to the growing body of research on IoT-enabled voting systems and their role in improving organizational and institutional decision-making.

Adrián Hložný, University of Zilina, Zilina, Slovakia (e-mail: hlozny3@stud.uniza.sk)
Michal Hodoň, University of Zilina, Zilina, Slovakia (e-mail: michal.hodon@fri.uniza.sk)
Lukáš Formanek, University of Zilina, Zilina, Slovakia (e-mail: lukas.formanek@fri.uniza.sk)

II. INTEGRATION

The methodology for the wireless voting system encompassed a comprehensive approach to integrating hardware, software, and communication protocols to create a robust, scalable, and user-friendly solution. The system comprises two primary components: voting devices and a collector device. Each voting device is designed to capture user input through tactile buttons that represent multiple-choice options and is powered by a rechargeable Li-Pol battery to ensure portability and independence from external power sources. The core of the voting device is the ESP32-WROOM-32D microcontroller, selected for its dual-core processing capability, low power consumption, and compatibility with the ESP-NOW protocol. This protocol allows for direct, low-latency wireless communication between devices without relying on an external WiFi network, simplifying deployment and enhancing reliability. The voting device encodes user inputs into compact data packets that include the device's unique identifier, the selected option, and a timestamp. These packets are then transmitted to the collector device using the ESP-NOW protocol. The collector device, also built around the ESP32 microcontroller, acts as the central processing unit of the system. It aggregates the data received from multiple voting devices and organizes it into an in-memory data structure that tracks the number of votes for each option. The collector device is configured to function as a web server, leveraging MicroPython's lightweight uHTTP library to host a dynamic and interactive user interface. This interface, developed using HTML, CSS, and JavaScript, provides real-time visualization of voting results in the form of bar graphs. The system's web interface is optimized for accessibility and responsive design, ensuring compatibility with various devices such as smartphones, tablets, and desktops. AJAX requests enable seamless updates to the displayed data without requiring manual page refreshes, further enhancing the user experience.

The hardware design incorporated several additional components to ensure stable and efficient operation. A TP4056 charging module manages the safe recharging of the Li-Pol battery, while an LM2596 DC-DC step-down converter regulates voltage to provide consistent power to the ESP32 module. This setup ensures reliable performance and extends the operational lifespan of the system. During the design phase, significant attention was given to the placement and configuration of components to minimize power consumption and maintain the compactness of the devices. The development process involved iterative testing and optimization to validate the system's functionality and performance. Reliability was tested by simulating simultaneous inputs from multiple voting devices, ensuring accurate data transmission and aggregation without packet loss. Latency was measured to confirm that the time between casting a vote and updating the visualization remained within acceptable limits for real-time operation. The energy efficiency of the voting devices was evaluated by monitoring battery performance under continuous use, confirming that the Li-Pol battery could sustain operation for extended periods. Scalability was another critical consideration, addressed by assigning unique identifiers to each voting device, allowing the system to accommodate additional devices without significant changes to its architecture.

The overall system architecture was designed with three functional layers: the input layer, comprising the voting devices; the processing layer, managed by the collector device; and the visualization layer, represented by the web-based user interface. These layers work in tandem to provide a seamless and intuitive voting experience. The input layer captures user selections, the processing layer ensures accurate aggregation and storage of data, and the visualization layer presents the results in a clear and accessible format. By integrating reliable hardware components, efficient communication protocols, and a responsive user interface, the methodology reflects a well-rounded approach to developing a practical and scalable wireless voting system that meets the needs of modern electronic voting scenarios.

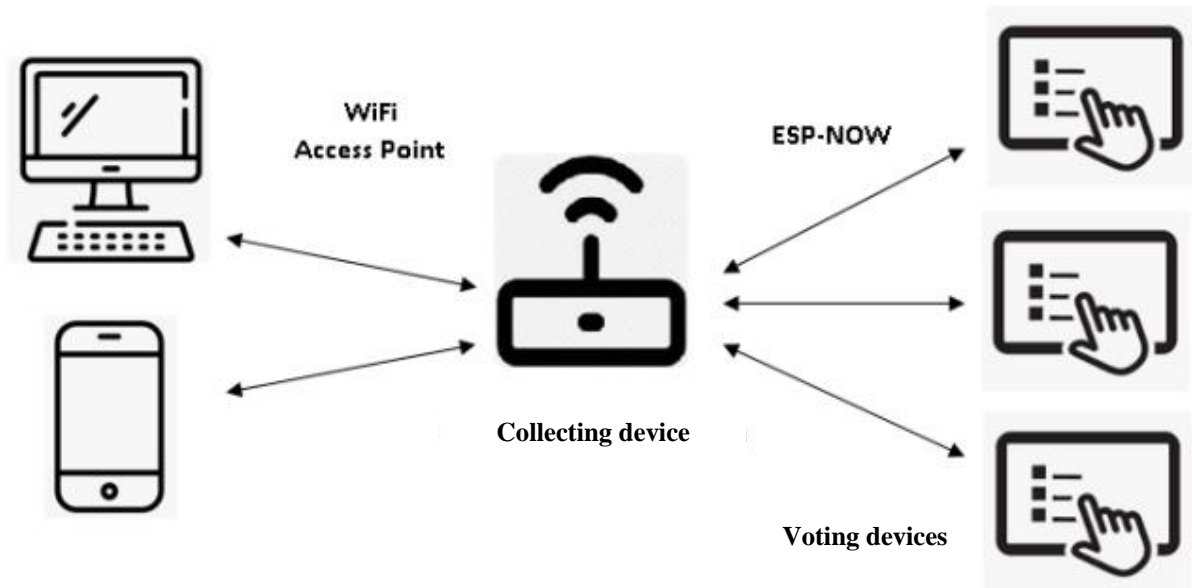


Fig. 1 System block schematic

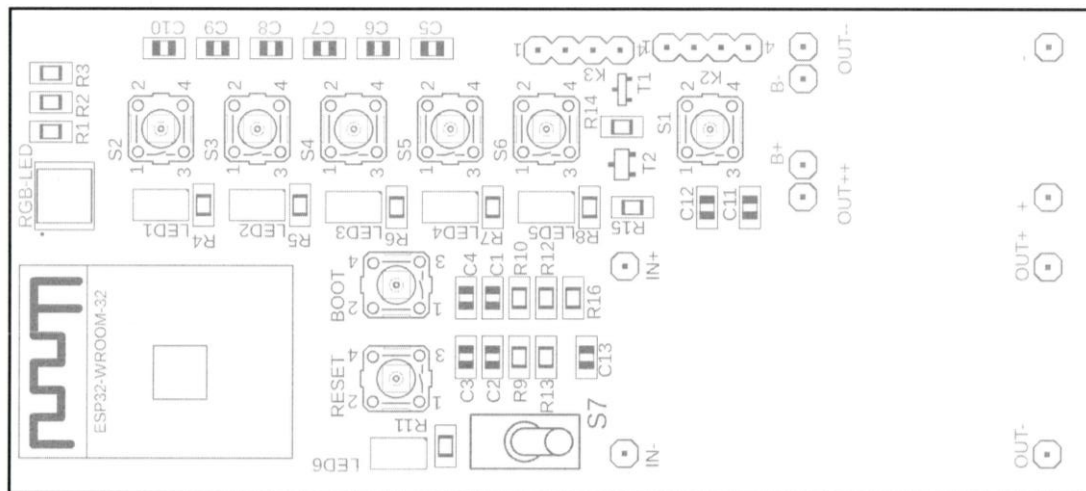


Fig. 2 Voting module

III. CONCLUSION

The system was tested in a controlled environment to evaluate its performance in terms of reliability, latency, and usability. The voting device successfully transmitted user selections to the collector device, which accurately processed and displayed the results. The bar graph visualization provided clear and immediate feedback on voting outcomes. Additionally, the system demonstrated low power consumption, with the Li-Pol battery sustaining extended operation under typical usage conditions. The ESP-NOW protocol proved effective, maintaining a stable connection between devices within the specified range. The proposed system offers several advantages over traditional voting methods, including faster data processing, reduced environmental impact, and enhanced user engagement. However, challenges such as signal interference and scalability limitations in larger environments highlight areas for improvement. Future enhancements could include integrating advanced encryption for data security, expanding the system's range, and developing a mobile application for easier access to the web interface. This study successfully implemented a wireless voting system using ESP32 technology. The system provides an efficient and cost-effective solution for electronic voting, with potential applications in education, business, and other domains.

Further research and development could explore scalability and additional features to enhance its utility in diverse settings.

REFERENCES

- [1] J. Bowen, "Digital solutions for transparent voting systems," *Journal of Electronic Governance*, vol. 8, no. 4, pp. 220-231, 2020.
- [2] S. Smith and A. White, "Sustainability challenges in modern voting practices," *Environmental Management Journal*, vol. 15, no. 2, pp. 112-119, 2021.
- [3] Espressif Systems, "ESP32 Technical Reference Manual," 2020. [Online]. Available: <https://www.espressif.com/en/support/documents>. [Accessed: Dec. 6, 2024].
- [4] R. Gupta and M. Singh, "IoT-based voting systems: A comprehensive review," *International Journal of Electronics and Communication*, vol. 12, no. 3, pp. 345-357, 2022.
- [5] A. Kumar, "Microcontroller innovations in wireless communication," *IEEE Micro*, vol. 34, no. 2, pp. 42-51, 2019.
- [6] Espressif Systems, "ESP-NOW protocol overview," 2022. [Online]. Available: <https://www.espressif.com/en/products/software/esp-now>. [Accessed: Dec. 6, 2024].
- [7] D. Wilson and L. Brown, "Low-latency communication for IoT applications," *IoT Journal*, vol. 9, no. 1, pp. 55-65, 2021.

Measurement of Muscle Signals and their Processing Using AI

Martin Uhrina, Michal Kubaščík, Ján Kapitulík

Abstract—The article focuses on monitoring and processing muscle activity signals using the MyoWare 2.0 sensor and the ESP32-P4 microcontroller. The MyoWare 2.0 sensor provides detailed electromyographic (EMG) data that can be processed in real time to analyze muscle performance, fatigue, or movement patterns. The ESP32-P4 microcontroller, equipped with advanced connectivity and built-in AI support, is used for data processing. Analog signals from the sensor are converted to digital form using an ADC and subsequently filtered to reduce noise. The microcontroller enables AI models, such as convolutional and recurrent neural networks, to classify gestures and monitor muscle fatigue. Processed data can be shared via Wi-Fi to cloud platforms like Google Firebase or ThingSpeak, locally using Bluetooth, or visualized on OLED or LCD displays. This approach integrates signal monitoring with artificial intelligence, offering practical applications in rehabilitation, robotics, and IoT.

Keywords—MyoWare 2.0, ESP32-P4, EMG signals, artificial intelligence, TensorFlow Lite, signal processing, Edge AI, IoT, Bluetooth, cloud platforms, OLED display

I. INTRODUCTION

Muscle activity is the fundamental driver of movement and communication in our body. The ability to capture and analyze the electrical signals generated by muscles can be applied in areas such as rehabilitation, sports performance, and the development of smart prosthetic technologies. These signals, recorded through electromyography (EMG), can reveal not only the intensity of muscle activity but also information about its condition, fatigue tolerance, and coordination with other muscles. Modern technology allows us not only to collect this data but also to process it efficiently.

The MyoWare 2.0 sensor is an advanced yet affordable tool for measuring muscle activity. With its compact design and easy integration with microcontrollers like the ESP32-P4, it allows for the integration of this data into artificial intelligence (AI)-driven applications. The ESP32-P4 is a next-generation microcontroller that combines high computational power with advanced peripherals. Thanks to its ability to process analog signals from the MyoWare sensor, apply filters to remove noise, and deploy AI models directly on the hardware, it represents an ideal platform for applications utilizing muscle signals. By combining artificial intelligence with EMG data, we can:

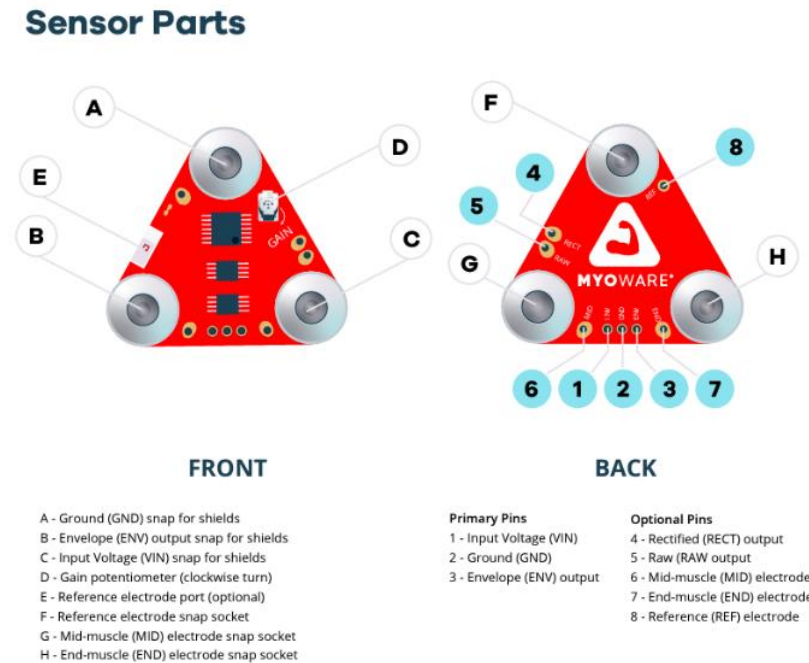
- Recognize complex movements or gestures for controlling robotic systems.
- Monitor muscle fatigue and prevent overloading during physical exertion.
- Analyze patient progress in rehabilitation in real-time.
- Create smart IoT devices that respond to muscle activity.

II. SENSOR MYOWARE 2.0

It is a sensor designed to detect and process surface electromyographic (sEMG) signals generated during muscle activity. When the brain communicates with muscles, it generates electrical signals that activate motor units, creating measurable electrical potentials. These

Martin Uhrina, University of Žilina, Slovak Republic (e-mail: uhrina@stud.uniza.sk)
Michal Kubaščík, University of Žilina, Slovak Republic (e-mail: michal.kubascik@fri.uniza.sk)
Ján Kapitulík, University of Žilina, Slovak Republic (e-mail: jan.kapitulik@fri.uniza.sk)

electrical signals are very weak, typically ranging from 2 to 10 mV in voltage. To give an idea of how such a signal works, we can use the example of bicep contraction. When the arm is extended and the bicep is relaxed, the electrical potential in the muscle will be very small, approximately 2 mV. However, when the muscle is contracted, the brain sends a more intense signal to the muscle, increasing the electrical potential in the muscle to about 10 mV.

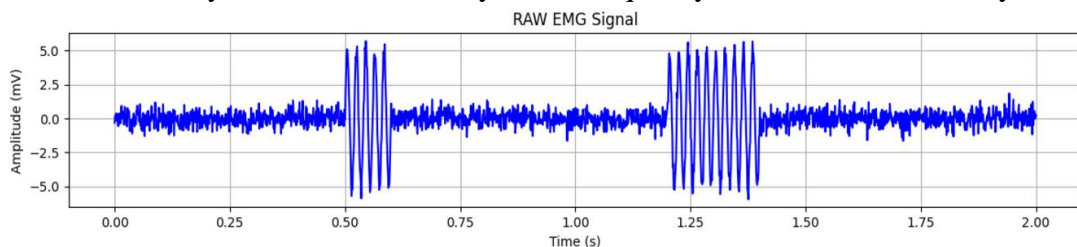


Picture 1 Sensor parts

The signal is measured by connecting three electrodes (MID, END, REF) to the muscle. The MID and END electrodes are used to measure the differential signal and are attached to a specific muscle, while the REF electrode provides a reference point located on a neutral part of the body, such as a bone.

A. RAW

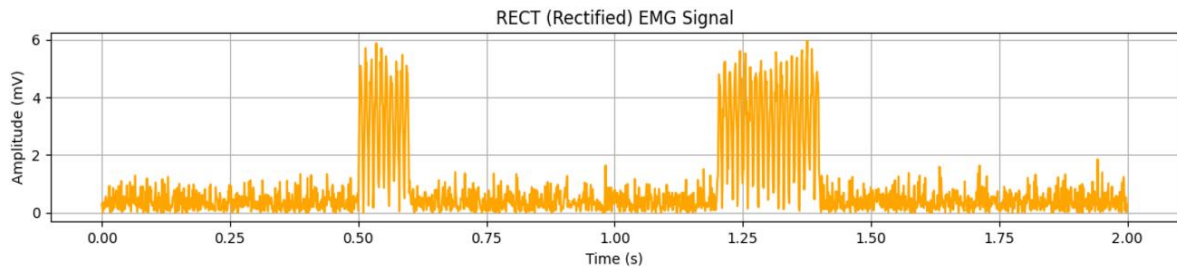
The raw output represents a 200-fold amplified and continuously monitored electrical signal from the muscles. It contains all the details about muscle activity, including high-frequency fluctuations and noise. This is an unprocessed signal. It typically ranges from 20 to 500 Hz, which corresponds to the physiological characteristics of sEMG signals. Such a signal can be used for detailed analysis of muscle activity or for frequency-based movement analysis.



Picture 2 Raw signal

B. RECT

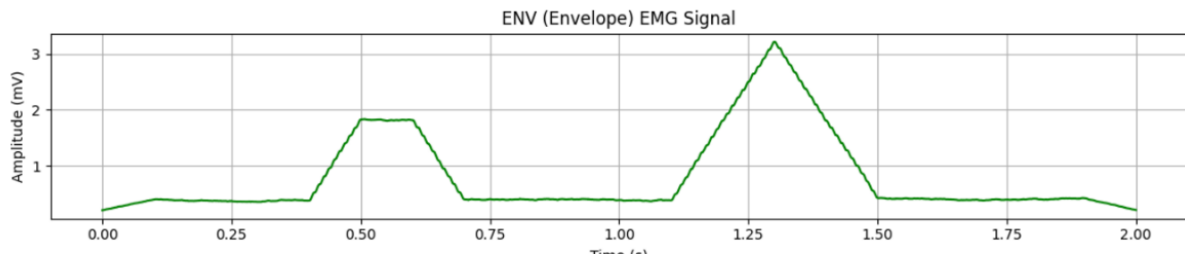
This signal represents the processed RAW signal, where all negative values are transformed into positive ones. This process is called full-wave rectification and ensures that the signal is easier to process. It is suitable for use in projects where advanced signal filtering is not required.



Picture 3 Rect signal

C. ENV

This output, the smoothed signal, represents the amplitude of muscle activity over time. Its calculation involves filtering high frequencies and applying a smoothing algorithm to remove minor fluctuations. It has a low frequency of approximately 3.6 Hz, which makes real-time processing easier. The amplification of this output can be adjusted using the potentiometer on the sensor. The amplification is calculated using the formula $G = 200 * R / 1k\Omega$. Since this output is suitable for real-time applications, it can be used in systems such as robotic control, prosthetic devices, or monitoring patient progress during rehabilitation.



Picture 4 ENV signal

III. USE OF ESP32-P4 FOR MONITORING MUSCLE ACTIVITY

To process the electrical signals from the MyoWare 2.0 sensor, we can use the ESP32-P4 microcontroller, a powerful device designed for applications that require rapid data analysis, advanced connectivity options, and artificial intelligence support. This microcontroller offers a wide range of communication interfaces, such as Wi-Fi 6, Bluetooth 5.0, SPI, UART, and I2C, ensuring flexibility when integrating into various systems. The ESP32-P4 not only allows for efficient processing of signals from the MyoWare 2.0 sensor but also facilitates sharing them across different platforms, making it ideal for modern applications in healthcare, sports, and IoT.

A. Sensor and Microcontroller Integration

For proper collaboration between the MyoWare 2.0 sensor and the ESP32-P4 microcontroller, their connection needs to be set up correctly. The MyoWare sensor provides three types of analog outputs (RAW, RECT, ENV), which can be connected to the analog input of the ESP32-P4. The microcontroller can then receive and process these signals.

The sensor can be powered directly from the microcontroller via either the 3.3 V or 5 V output, depending on the requirements.

Once the signal is received at the analog input of the ESP32-P4, it is converted to a digital form using an ADC (Analog-to-Digital Converter). This process allows the microcontroller to further process the acquired data. The ESP32-P4 can apply programmable filters to remove noise and highlight the desired signal. For example, a low-pass filter isolates the ENV signal, while a high-pass filter can remove certain interferences.

To read data from the ADC on the ESP32-P4, we can use the driver/adc library, which allows for the configuration of ADC channels, real-time reading of analog signals, and continuous

sampling using DMA. For more advanced signal analysis and processing, such as filtering, libraries like ESP-DSP or CMSIS-DSP can be used, offering a wide range of tools for digital signal processing.

B. Processing Measured Data Using AI

The ESP32-P4 microcontroller has built-in support for artificial intelligence, enabling signal processing directly on the device using the Edge AI method. This signal processing approach reduces reliance on cloud services, thereby speeding up data processing.

After the signal is received via the ADC converter, preprocessing is required. First, filters are applied to clean the data of noise, and then the signal values are adjusted to an appropriate range for processing by an AI model. Convolutional Neural Networks (CNNs) or Recurrent Neural Networks (RNNs) can be used for such signal processing. Convolutional networks are ideal for recognizing patterns, gestures, or movements, while recurrent networks are more suitable for monitoring muscle fatigue or analyzing time-series data.

To implement AI models on the ESP32-P4 microcontroller, libraries such as TensorFlow Lite for Microcontrollers and uTensor can be used. These libraries enable the deployment of pre-trained AI models directly onto the microcontroller, which is ideal for devices with limited computational power. uTensor, like TensorFlow Lite, is designed to efficiently run models on low-power devices. Additionally, libraries like ESP-DSP and CMSIS-DSP can be utilized.

AI models can identify various muscle movements, such as hand flexion, finger contraction, or grip, making them ideal for controlling robotic devices. Furthermore, they can be used to detect muscle fatigue, such as by monitoring the drop in signal amplitude during exercise or other physical activities.

C. Sharing Measured Data

The measured signal and processed data can be shared across various platforms for better representation. Using Wi-Fi, these data can be sent to cloud storage services like Google Firebase, AWS IoT Core, ThingSpeak, or to a private server. This allows for long-term archiving, easy access, and later analysis.

For local communication with mobile applications, the Bluetooth interface can be used. ESP-IDF provides the `esp_ble_gatts` library, which allows the creation of a Bluetooth server for sending real-time data.

For local display, we can use a screen connected via I2C or SPI, where we can display the measured signals or processed results. For working with OLED displays, libraries like Adafruit SSD1306 or U8g2 can be used, which are powerful and provide flexible graphical display options.

Table 1 Methods of Sharing

| Method of Sharing | Advantages | Disatvantages |
|-------------------|--------------------------------|-----------------------------------|
| Cloud(Wi-Fi) | Global access to data | Requires internet connect |
| Bluetooth | Local sharing(mobile app) | Limited range (approx. 10 meters) |
| OLED/LCD display | Direct display from the device | Limited space for detailed data |

IV. CONCLUSION

The integration of advanced sensing technologies, such as the MyoWare 2.0 sensor, with the versatile capabilities of the ESP32-P4 microcontroller represents a significant step forward in muscle signal monitoring and analysis. This combination allows for real-time data processing and the application of artificial intelligence directly on embedded devices, reducing reliance on external computing resources. By leveraging machine learning models, it becomes possible to classify gestures, detect muscle fatigue, and enable innovative applications in fields such as

rehabilitation, robotics, and IoT.

Additionally, the flexibility in sharing measured and processed data—whether via cloud storage, Bluetooth communication, or direct visualization on a display—ensures usability in diverse environments. Despite the challenges of limited hardware resources, the use of optimized libraries like TensorFlow Lite and ESP-DSP demonstrates the feasibility of deploying powerful AI tools on embedded platforms. Future work could focus on expanding the range of AI models, improving signal accuracy, and integrating the system into more comprehensive healthcare and robotic systems, further unlocking the potential of electromyographic analysis in practical applications.

REFERENCES

- [1] "SparkFun 9DoF IMU Breakout - MPU9250," *SparkFun Electronics*. [Online]. Available: <https://www.sparkfun.com/products/21265>. [Accessed: Dec. 6, 2024].
- [2] "Myoware Muscle Sensor," *Myoware*. [Online]. Available: <https://myoware.com/products/muscle-sensor/>. [Accessed: Dec. 6, 2024].
- [3] "SparkFun DEV-18977 Product Overview," *Mouser Electronics*. [Online]. Available: <https://www.mouser.com/pdfDocs/Productoverview-SparkFun-DEV-18977.pdf>. [Accessed: Dec. 6, 2024].
- [4] Espressif Systems, "ESP-DSP," GitHub Repository. [Online]. Available: <https://github.com/espressif/esp-dsp>. [Accessed: Dec. 6, 2024].
- [5] "SparkFun 9DoF IMU Breakout - LSM9DS1," *SparkFun Electronics*. [Online]. Available: <https://www.sparkfun.com/products/21269>. [Accessed: Dec. 6, 2024].
- [6] Espressif Systems, "ESP32-P4 Function EV Board User Guide," *Espressif Systems*. [Online]. Available: https://docs.espressif.com/projects/esp-dev-kits/en/latest/esp32p4/esp32-p4-function-ev-board/user_guide.html. [Accessed: Dec. 6, 2024].
- [7] Espressif Systems, "ESP32-P4," *Espressif Systems*. [Online]. Available: <https://www.espressif.com/en/news/ESP32-P4>. [Accessed: Dec. 6, 2024].
- [8] Espressif Systems, "ESP-TFLite Micro," GitHub Repository. [Online]. Available: <https://github.com/espressif/esp-tflite-micro>. [Accessed: Dec. 6, 2024].
- [9] Eloquent Arduino, "TensorFlow Lite on ESP32 for TinyML," *Eloquent Arduino*. [Online]. Available: <https://eloquentarduino.com/posts/tensorflow-lite-tinyml-esp32>. [Accessed: Dec. 6, 2024].

System for Quality of Traffic Infrastructure Measurements

Miloslav Slodičák, Michal Hodoň, Juraj Miček, Peter Ševčík

Abstract—This paper presents the development of a system designed to evaluate the quality of traffic infrastructure by integrating a custom-built sensor prototype with an Android application. The system leverages sensor data to detect road surface irregularities, providing users and authorities with actionable insights. The sensor module records acceleration and vibration data, which are processed to identify critical road conditions. A mobile application visualizes this data in real time, enhancing user interaction and data accessibility. This work outlines the hardware and software design, experimental validation, and potential applications in traffic monitoring and urban planning.

Keywords—Traffic infrastructure, road quality monitoring, sensor prototype, Android application, IoT.

I. INTRODUCTION

The quality of traffic infrastructure directly influences safety, vehicle maintenance costs, and the overall efficiency of transportation networks. Poor road conditions, including potholes, uneven surfaces, and structural degradation, can lead to accidents, increased fuel consumption, and higher maintenance expenses for vehicles. As urbanization accelerates, maintaining road infrastructure has become a critical priority for municipalities and governments worldwide. Effective monitoring systems are essential for identifying problematic areas, prioritizing repairs, and optimizing resource allocation [1][2]. Traditional methods of assessing road quality rely heavily on manual inspections or specialized vehicles equipped with expensive instrumentation, such as high-resolution cameras, laser scanners, and accelerometers. These approaches, while accurate, are labor-intensive, costly, and limited in scalability. Manual inspections are subject to human error and cannot provide real-time or large-scale data. On the other hand, specialized vehicles, though effective, are often constrained by their high operational costs and dependency on trained personnel [3]. Consequently, there is a growing demand for more accessible and scalable solutions that leverage modern technologies to monitor traffic infrastructure efficiently. The emergence of Internet of Things (IoT) technologies has introduced a transformative approach to infrastructure monitoring. IoT devices, characterized by their low cost, portability, and connectivity, offer significant advantages in scalability and real-time data acquisition. Recent advancements in microcontrollers, sensors, and mobile applications have enabled the development of systems that can collect, process, and visualize data on road quality using everyday vehicles as data collectors. For example, systems like Pothole Patrol and SmartRoads have demonstrated the feasibility of using accelerometers and GPS-equipped smartphones for detecting road anomalies. However, these solutions face challenges in data accuracy due to noise from vehicle-specific factors and environmental conditions [4][5]. This study introduces a cost-effective system for monitoring traffic infrastructure quality using a custom-built sensor prototype and an Android application. The sensor module combines an MPU-6050 accelerometer and gyroscope with an ESP32 microcontroller for data acquisition and processing. The Android application provides real-time visualization, geolocation integration, and user interaction

Miloslav Slodičák, University of Zilina, Zilina, Slovakia (e-mail: slodicak@stud.uniza.sk)
Michal Hodoň, University of Zilina, Zilina, Slovakia (e-mail: michal.hodon@fri.uniza.sk)
Juraj Miček, University of Zilina, Zilina, Slovakia (e-mail: juraj.micek@fri.uniza.sk)
Peter Ševčík, University of Zilina, Zilina, Slovakia (e-mail: peter.sevcik@fri.uniza.sk)

features. The system leverages Bluetooth Low Energy (BLE) communication for efficient data transmission and integrates GPS data to map road conditions across different locations. Unlike existing systems, the proposed solution emphasizes ease of deployment, portability, and user accessibility, making it suitable for both individual users and municipal authorities.

In addition to addressing the limitations of traditional methods, the proposed system incorporates state-of-the-art advancements in IoT and sensor technology to enhance data accuracy and reliability. The MPU-6050, a widely used motion tracking sensor, offers precise acceleration and angular velocity measurements, enabling the detection of subtle road irregularities. The ESP32 microcontroller facilitates real-time processing and seamless communication with the mobile application. Furthermore, the system's modular architecture allows for scalability and integration with advanced data analytics tools, such as machine learning algorithms, to predict infrastructure deterioration trends [6][7]. This paper outlines the design, implementation, and validation of the system, highlighting its potential applications in traffic management, urban planning, and predictive maintenance. By combining real-time data acquisition with intuitive visualization, the system aims to democratize access to road quality information, enabling users to actively participate in infrastructure monitoring and decision-making.

II. INTEGRATION

The methodology for developing the traffic infrastructure quality monitoring system focused on integrating hardware and software components into a functional, scalable, and user-friendly solution for road condition assessment. The system's core hardware comprises an MPU-6050 accelerometer and gyroscope module, an ESP32 microcontroller, and a rechargeable battery, all housed within a compact and portable casing. The MPU-6050 module was selected for its ability to provide precise acceleration and angular velocity measurements, essential for detecting vibrations and motion patterns indicative of road irregularities. The ESP32 microcontroller, chosen for its processing power and Bluetooth Low Energy (BLE) capabilities, handles data acquisition, processing, and communication with the Android application. The rechargeable Li-Pol battery powers the system, ensuring portability and extended operational duration. The hardware design emphasized modularity, allowing for easy replacement or upgrading of individual components without affecting the overall functionality of the system.

The software for the sensor prototype was developed using the Arduino IDE, with a focus on real-time data acquisition and processing. The ESP32 microcontroller collects raw data from the MPU-6050 sensor at predefined intervals, filters out noise using a low-pass filter, and calculates key metrics such as vibration intensity and orientation deviations. These metrics are processed to identify road conditions that fall into predefined categories such as smooth, moderate, or poor. The processed data is then packaged and transmitted to the Android application via BLE. To ensure reliability and reduce latency, the BLE communication protocol was optimized to minimize packet loss and maximize transmission speed. The Android application, developed using Kotlin in Android Studio, interfaces with the sensor prototype to visualize real-time data and provide geolocation-based mapping of road conditions. The application integrates GPS functionality to associate sensor readings with specific locations, creating a spatially resolved map of road quality. Additional features include user logging capabilities, allowing individuals to manually tag specific road events such as potholes or construction zones, enhancing the system's data granularity.

System integration was achieved by establishing a seamless communication pipeline between the sensor prototype and the Android application. The microcontroller continuously streams data to the mobile device, where it is displayed using graphical tools, including line graphs and

heat maps, to offer intuitive insights into road conditions. The modular architecture of the system enables scalability, allowing multiple sensor prototypes to operate concurrently and send data to the same application for broader area coverage. Testing and calibration were integral to the development process, with extensive evaluations conducted in controlled and real-world environments. Calibration ensured that the MPU-6050 sensor accurately measured acceleration and angular velocity, while thresholds for vibration intensity were fine-tuned to distinguish between normal vehicle motion and road surface irregularities. Real-world tests involved driving over various road types to assess the system's performance in detecting and categorizing road quality accurately. Power efficiency was another critical aspect addressed during the development process. The ESP32 microcontroller's sleep modes were utilized to reduce power consumption during periods of inactivity, extending the operational life of the battery. Additionally, the Android application was optimized to minimize resource usage while maintaining responsiveness and functionality. Challenges encountered during development included handling environmental noise and external vibrations unrelated to road conditions, which were mitigated using software-based filtering techniques. The methodology ensured a robust, portable, and cost-effective solution that combines accurate road quality assessment with intuitive visualization, making it suitable for diverse applications in traffic monitoring, urban planning, and infrastructure maintenance. Future iterations of the system could integrate machine learning algorithms to further enhance data classification and provide predictive analytics for proactive infrastructure management.

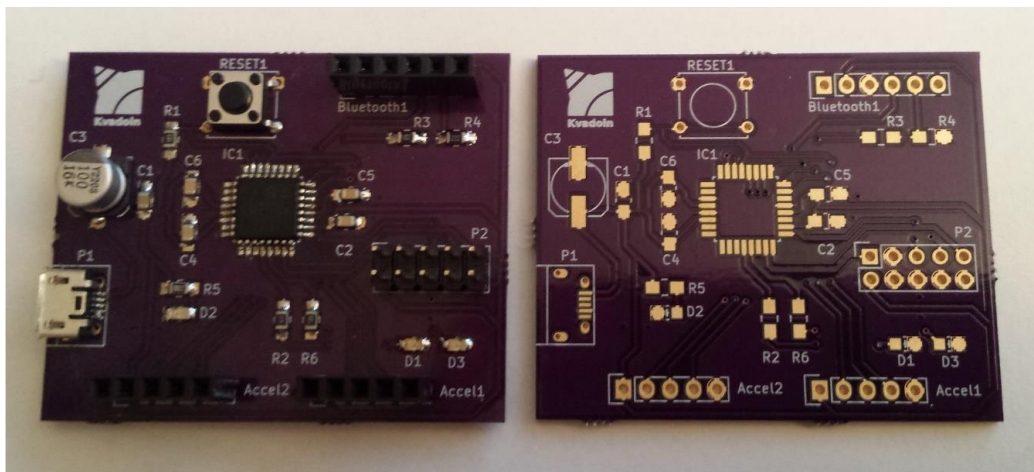


Fig. 1 Developed device

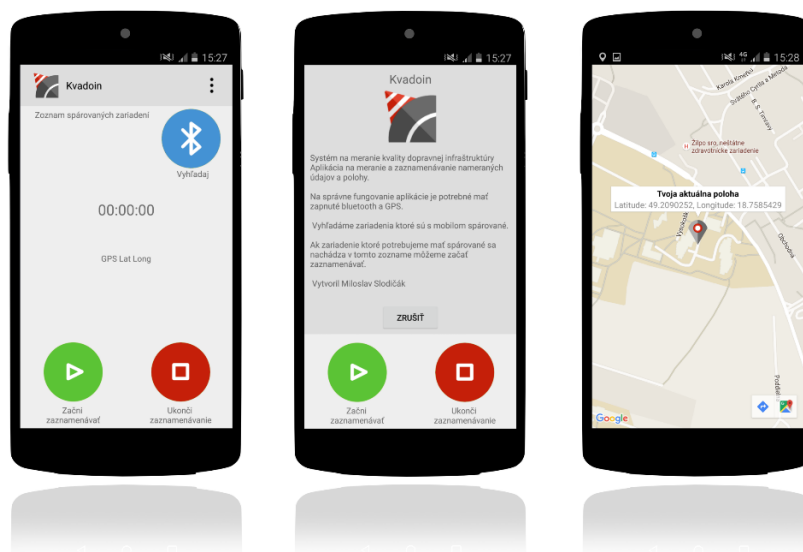
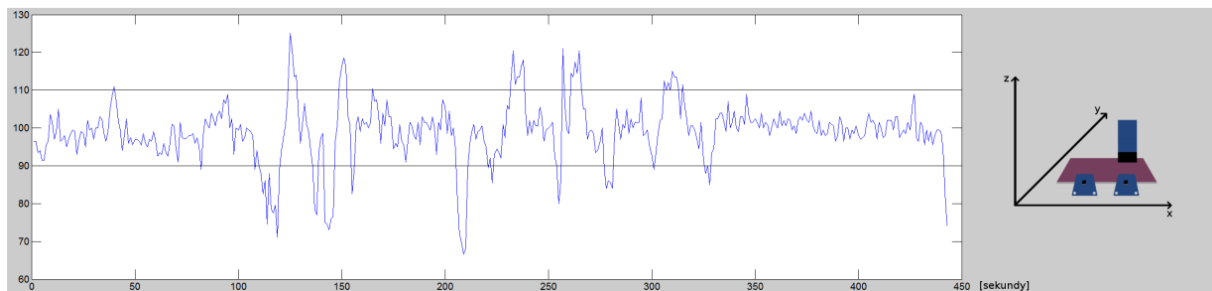


Fig. 2 Graphical interface



Fig. 3 Measurement scenario

Fig. 4 Measured results on the 1st class highway route 66

III. CONCLUSION

The system was tested in various real-world conditions, including urban streets and highways. The sensor module successfully detected road surface irregularities with a high degree of accuracy, correlating with manually observed conditions. Bluetooth communication between the sensor and the application remained stable across different environments, with minimal data loss. The Android application provided clear and actionable insights, with users reporting high satisfaction in terms of ease of use and responsiveness. Experimental results demonstrated the system's ability to classify road conditions into categories, such as smooth, moderate, and poor, based on vibration intensity metrics. The proposed system offers a cost-effective and scalable solution for road quality monitoring, addressing limitations of traditional methods. By leveraging widely available hardware components and an intuitive mobile application, the system democratizes access to road condition data. However, certain challenges remain, including sensor sensitivity to external vibrations unrelated to road quality (e.g., vehicle-specific factors) and potential connectivity issues in dense urban areas. Future iterations could incorporate machine learning algorithms to enhance data classification and expand functionality to include additional metrics, such as noise pollution. This study successfully developed and validated a system for monitoring traffic infrastructure quality. The integration of a custom sensor module and an Android application provides a portable, accessible, and scalable solution for identifying and addressing road surface irregularities. The system has significant potential applications in urban planning, road maintenance, and traffic management,

offering insights that can improve safety and efficiency on roads. Future research could explore enhancing system robustness and integrating advanced analytics for predictive maintenance.

REFERENCES

- [1] J. Gubbi, R. Buyya, S. Marusic, and M. Palaniswami, "Internet of Things (IoT): A Vision, Architectural Elements, and Future Directions," *Future Generation Computer Systems*, vol. 29, no. 7, pp. 1645-1660, 2013.
- [2] J. Bowen, "Digital Solutions for Asset Security in Logistics," *Journal of Logistics Management*, vol. 18, no. 4, pp. 321-334, 2020.
- [3] Espressif Systems, "ESP32 Technical Reference Manual," 2020.
- [4] L. Atzori, A. Iera, and G. Morabito, "The Internet of Things: A Survey," *Computer Networks*, vol. 54, no. 15, pp. 2787-2805, 2010.
- [5] InvenSense, "MPU-6050 Datasheet," 2023.
- [6] A. Kumar, "IoT-Based Security Solutions: Challenges and Opportunities," *IEEE Internet of Things Journal*, vol. 8, no. 2, pp. 245-258, 2021.
- [7] G. Fersi, "IoT-Based Electronic Seals: Enhancing Security in Logistics," *Journal of Innovation in Digital Systems*, vol. 15, no. 2, pp. 98-107, 2022.
- [8] R. Gupta and P. Singh, "Energy-Efficient IoT Security Systems," *Journal of Embedded Systems*, vol. 12, no. 4, pp. 245-259, 2022.

Sustainability of the 3D Printing Laboratory Operation on Faculty of Management Science and Informatics University of Žilina

Lukáš Čechovič, Marek Tebeľák, Michal Kubaščík, Juraj Miček

Abstract—“This paper focuses on the integration of sustainability into the educational process through the subject of 3D printing. Over recent years, 3D printers have become accessible to a broad public due to their affordability, user-friendliness, and reliability. In 2019, we introduced 3D printing as a subject at the Faculty of Management Science and Informatics University of Žilina with the goal of making it accessible to all students, regardless of their field of study. This multidisciplinary technology allows students to unleash their creativity and broaden their perspectives. The 3D printing process captivates students as they transform their ideas into tangible objects. Starting with a concept, they use CAD software for modeling and finalize their creations with a physical product—all within a single lesson. This hands-on approach has made the subject highly popular, leading to increased student participation and engagement. This paper emphasizes the importance of integrating sustainable practices into the 3D printing curriculum. Specifically, it explores strategies for recycling and reusing materials used during practical lessons to minimize waste and reduce the environmental impact. By promoting a circular approach to material usage, the subject aims to instill an awareness of sustainability in students. The paper also discusses the process of selecting appropriate technical equipment for the laboratory to support effective recycling of materials used in 3D printing. Ensuring student safety and the reliability of the equipment remains a priority, but the emphasis is placed on integrating tools and devices that enable the collection, processing, and reuse of waste materials, such as failed prints or support structures. This paper recommends that 3D printing, combined with sustainable practices, should become a fundamental component of education across various disciplines and institutions. [3]

Keywords— 3D printing, filament, sustainability, laboratory

I. INTRODUCTION

Through the process of learning how to design your own models and print them, you may encounter difficulties, which can result in plastic scraps such as support materials and failed prints. For years, it has been common practice to throw this scrap away, but as the issue of microplastics and plastic waste pollution becomes more relevant. As plastic materials degrade, they break into smaller pieces and are harder to eliminate. It has been proven that microplastics are even present in our bloodstreams and may cause many unwanted and harmful effects on the immune system and body.

In 2019, the Faculty of Management Science and Informatics in University of Žilina introduced 3D printing as a course with the goal of making it accessible to all students, regardless of their field of study. This multidisciplinary technology allows students to unleash their creativity and broaden their perspectives. Although it is good to teach people new things, their learning process may be slow and riddled with mistakes that create plastic products no longer usable under normal circumstances unless recycled.

Since the 3D printing subject began operating, we have been collecting plastic waste from 3D printers with the intention of recycling it to produce our own filament. To further this goal, we are considering the purchase of a recycler. Additionally, we are working on developing our own version of the recycler in collaboration with students.

Recycling is one way to introduce sustainability into the learning and practices of students and 3D printing enthusiasts. It has many benefits, not only for nature, but also for finances and

Lukáš Čechovič, University of Žilina, Žilina, Slovakia (e-mail: lukas.cechovic@fri.uniza.sk)
Marek Tebeľák, University of Žilina, Slovak Republic (e-mail: tebelak2@stud.uniza.sk)
Michal Kubaščík, University of Žilina, Slovak Republic (e-mail: michal.kubascik@fri.uniza.sk)
Juraj Miček, University of Žilina, Slovak Republic (e-mail: juraj.micek@fri.uniza.sk)

overall self-sufficiency in this field. Unfortunately, due to the laws of nature, there is no way to achieve 100% self-sufficiency or 100% recycling of waste. However, through trial and error and working together, people have managed to create many thriving communities that collect waste plastic and repurpose it for new uses.

In the course on 3D printing in 2024, 255 grams of filament were used per student group. There were 138 groups in 2024, which amounts to a total consumption of 35,3175 kilograms of filament for the entire semester.

II. PROPOSED TECHNICAL EQUIPMENT

For the purposes of analysis in this article, we will use two different models of filament recyclers: Felfil and Filabot.

A. *Filabot EX2* [2]

- **Build Quality:** The Filabot EX2 has a robust, all-metal frame
- **Temperature Range:** It can reach up to 329°C, allowing it to handle a variety of materials including PLA, ABS, PETG, HIPS
- **Extrusion Speed:** The EX2 producing up to 907g of filament per hour
- **Filament Tolerance:** It maintains a diameter tolerance of +/- 0.05 mm
- **Price:** starts at 19000 eur (Extruder, Spooler, Shredder)

B. *Felfil Evo* [1]

- **Build Quality:** The Felfil Evo is available as both a pre-assembled unit and a DIY kit
- **Temperature Range:** It can heat up to 30°C, which is sufficient for materials like PLA, PETG, ABS, HIPS, and TPU
- **Extrusion Speed:** The Evo has extrusion rate of 100-150 grams per hour
- **Filament Tolerance:** It has a tolerance of +/- 0.07 mm
- **Ease of Use:** The Evo is relatively easy to assemble and use, especially for beginners
- **Price:** 2700 eur (Extruder, Spooler, Shredder)

Filabot EX2 is more suitable for users needing higher extrusion speeds and a wider range of material compatibility. **Felfil Evo** is a cost-effective option for those who are okay with slower speeds and need a simpler setup.

III. RECYCLING RATIOS OF NEW AND RECYCLED MATERIAL FOR FDM 3D PRINTING FILAMENT

The ratio of new to recycled material in FDM 3D printing filament depends on the quality of the recycled filament, the recycling technology used, and the requirements for the final prints [4], [5], [6]. Typical ratios fall within the following ranges:

A. *70% New / 30% Recycled Material*

- The most commonly used ratio for recycling.
- Ensures good quality and mechanical properties of the filament.
- The new material adds stability and consistency to the filament, preventing printing issues such as poor layer adhesion or print failures.

B. *50% New / 50% Recycled Material*

- A balanced ratio used when the recycled material is well-processed (uniform granules, free of impurities).
- Mechanical properties may be slightly reduced but remain sufficient for many common applications, such as prototypes or decorative objects.

C. 30% New / 70% Recycled Material

- Less common but feasible when using high-quality recycled filament.
- Mainly used for low-demand models or applications where high strength and precision are not critical.
- Requires careful quality control of the recycled material.

D. 100% Recycled Material

- The most challenging option, as recycled filament may suffer from instability and reduced quality (inconsistent diameter, weaker mechanical properties).
- Suitable only for experimental applications or when specialized recycling equipment is available.
- Not recommended for precise prints or critical functional parts.

E. Factors Affecting the Ratio

1. Material Type: PLA and PETG are easier to recycle, whereas ABS or nylon require more advanced processing techniques.
2. Recycling Quality: Proper granulation and re-extrusion processes are crucial to avoid impurities and polymer degradation.
3. Printing Purpose: Higher recycled content is acceptable for decorative objects, whereas functional parts require a higher proportion of new material.

The optimal ratio depends on the specific project requirements, but for most applications, a 70% new to 30% recycled material ratio is recommended to ensure good print quality and stability.

IV. PREFERRED MATERIAL TYPE

PLA (Polylactic Acid) is the material used in our 3D printing education process. The advantages of **PLA** make it the ideal choice. PLA is made from renewable resources like cornstarch or sugarcane, which aligns with our sustainability goals. Its **ease of use** and **low melting point** allow students to work with it confidently, reducing print issues like warping and ensuring reliable results. Additionally, **PLA is non-toxic**, making it safe for educational environments, as it doesn't release harmful volatile organic compound (VOC) during printing. Finally, the **high-quality finish** and **detail** it produces are perfect for student projects, prototypes, and visual demonstrations. These characteristics make PLA the ideal filament for use exclusively in the educational process.

A. The price of PLA pellets

The price of PLA pellets for recycling into filament varies depending on the source and material quality. Generally:

1. New PLA Pellets: These cost approximately 200eur for a 25 kg bag, which translates to about 8eur per kilogram. These are high-quality pellets used for professional-grade filaments and 3D printing applications [7].

2. Recycled PLA Pellets (rPLA): These are often more environmentally friendly and may cost slightly less. They are typically produced from recycled PLA waste and are available in various colors and formulations. Specific prices depend on the supplier and batch availability, as recycled materials can fluctuate in price due to sourcing challenges

B. Calculations

The following table calculates the cost of producing 1 kg of recycled filament at various ratios of new to old material, assuming the cost of new material is €8/kg, and the old material is considered free (€0/kg):

Table 1. Price of production

| Ratio of New/Old Material | Cost of New Material (€) | Cost of Old Material (€) | Cost per 1 kg of Recycled Filament (€) |
|----------------------------------|---------------------------------|---------------------------------|---|
| 100% New / 0% Old | 8.00 | 0.00 | 8.00 |
| 70% New / 30% Old | 5.60 | 0.00 | 5.60 |
| 50% New / 50% Old | 4.00 | 0.00 | 4.00 |
| 0% New / 100% Old | 0.00 | 0.00 | 0.00 |

The cost of old material in our scenario is zero, as we have collected enough old material over the previous years of laboratory functioning. Cost per 1 kg of filament = (Proportion of new material × cost of new material) + (Proportion of old material × cost of old material). A higher proportion of recycled material significantly reduces the overall production costs.

Here's a comparative table of the additional costs and time required to produce 1 kg of filament using the Felfil EVO and Filabot EX2 extruders:

Table 2. Additional costs

| Extruder | Production Rate (kg/hour) | Power Consumption (W/hour) | Time to Produce 1 kg (hours) | Energy Cost (€/kWh) | Cost to Produce 1 kg (€/kg) | Notes |
|--------------------|----------------------------------|-----------------------------------|-------------------------------------|----------------------------|------------------------------------|---|
| Felfil EVO | 0.15 | 80 | 6.67 | 0.20 | 0.107 | Low production rate |
| Filabot EX2 | 0.907 | 500 | 1.10 | 0.20 | 0.11 | High production rate, suitable for large-scale recycling operations. |

Felfil is slower, making it ideal for small-scale or hobbyist recycling. Filabot EX2 is faster and better suited for industrial or large-scale use, offering higher productivity.

To calculate how long it would take to produce 35.3175 kg (annual consumption) of filament using the Felfil EVO and Filabot EX2 extruders, we use their production rates:

1. Felfil:

- o Production rate: 0.15 kg/hour
- o Felfil: Approximately 235.5 hours to produce 35.3175 kg of filament.

2. Filabot EX2:

- o Production rate: 0.907 kg/hour
- o Filabot EX2: Approximately 38.9 hours to produce 35.3175 kg of filament.

Table evaluating various ratios, cost savings, and the payback period for the proposed recycling machines.

Table 3. Evaluations

| Device | Price (€) | Recycling Ratio (New:Recycled) | Cost per kg (€) | Electricity Cost (€) | Total Cost per kg (€) | Savings per kg (€) | Savings on 35.3175 kg (€) | Payback Period (kg) |
|--------------------|-----------|--------------------------------|-----------------|----------------------|-----------------------|--------------------|---------------------------|---------------------|
| Felfill | 2,700 | 50:50 | 4.00 | 0.10 | 4.10 | 25.90 | 916.42 | 104.00 |
| | | 70:30 | 5.60 | 0.10 | 5.70 | 24.30 | 858.61 | 111.59 |
| | | 100:0 | 8.00 | 0.10 | 8.10 | 21.90 | 773.59 | 122.45 |
| | | 0:100 | 0.00 | 0.10 | 0.10 | 29.90 | 1,057.88 | 90.00 |
| Filabot EX2 | 19,000 | 50:50 | 4.00 | 0.10 | 4.10 | 25.90 | 916.42 | 733.59 |
| | | 70:30 | 5.60 | 0.10 | 5.70 | 24.30 | 858.61 | 781.89 |
| | | 100:0 | 8.00 | 0.10 | 8.10 | 21.90 | 773.59 | 867.57 |
| | | 0:100 | 0.00 | 0.10 | 0.10 | 29.90 | 1,057.88 | 635.45 |

The Felfill extruder has a faster payback period due to its lower initial cost, achieving breakeven after producing between **90.56 to 123.86 kg** of filament, depending on the recycling ratio. Based on the estimated **annual filament consumption of 35.3175 kg** in 2024, the Felfill would reach payback in approximately **2.6 to 3.5 years**.

The Filabot EX2, while more expensive, benefits from industrial-scale production, and would require **636.45 to 870.64 kg** of filament to break even, assuming lower production costs. With **35.3175 kg** of filament production annually, the Filabot EX2 would require **18.0 to 24.7 years** to achieve payback.

C. Cost of Replacing Components:

Felfil Common parts like **nozzles** and **feed gears** can cost around **€10–€100** depending on the part, and replacing worn-out components may incur these costs annually. **Filabot EX2** replacement parts like **motors** or **heating elements** can cost upwards of **€200–€500** for major components. Regular parts replacements can range between **€300–€700** annually, depending on usage and how aggressively the machine is used.

V. DISCUSSION

The Felfill Evo is priced at €2,700, making it significantly more affordable compared to industrial-scale machines like the Filabot EX2 priced at €19,000. This lower cost is especially important for educational and research environments where budget constraints are common.

The Felfill extruder produces 0.15 kg of filament per hour, which aligns well with the laboratory's material consumption of approximately 35.3175 kg per year. Given that the demand for filament is not extremely high, this machine can meet the needs without unnecessary excess capacity. In comparison, the Filabot EX2 can produce 0.907 kg per hour, making it more suitable for industrial-scale operations, but its higher production capacity would be underutilized in a laboratory setting, potentially leading to inefficient use of resources.

The Felfill Evo has a much faster payback period compared to the Filabot EX2, which would result in quicker cost recovery. For a recycling ratio of 50:50, the payback period for Felfill is around 3 years. In contrast, the Filabot EX2 would take approximately 21 years to recover its initial investment at the same recycling ratio. Considering the laboratory's material needs, the Felfill Evo's smaller scale allows it to achieve a payback period within a reasonable timeframe, ensuring cost efficiency without excessive upfront expenditure. Without including labor costs, the payback periods are significantly shorter for the Felfill extruder, which reaches payback in approximately 3 years (depending on the recycling ratio). In contrast, the Filabot EX2 requires 21 years to break even, reflecting its higher initial cost and less favorable payback profile.

The Felfill Evo's simpler setup and operation make it ideal for educational environments, where students can directly engage with the recycling process, learn about filament production, and experiment with various recycled materials. The low operational and maintenance costs further enhance its fit for the lab's needs.

In this case, we will exclude the labor costs for operating the machines since it is assumed that the devices will be operated by students as part of their educational process. This means that we will focus on material and service costs only for the calculations.

Based on the material needs of the 3D printing laboratory at the Faculty of Management Science and Informatics (FRI UNIZA), it appears that a device with a lower initial cost and smaller production capacity, such as the Felfill extruder (Felfill Evo), would be a more suitable choice for the laboratory's scale.

VI. CONCLUSION

Given the relatively modest filament requirements at the FRI UNIZA 3D printing laboratory, coupled with budget constraints and educational goals, the Felfill Evo offers a more cost-effective and appropriate solution. Its lower initial cost, sufficient production capacity, and faster payback period make it a suitable choice for meeting the laboratory's needs efficiently, while avoiding the excess capacity and high costs associated with larger machines like the Filabot EX2.

This analysis suggests that investing in smaller-scale filament recycling machines like Felfill Evo aligns well with the laboratory's goals, allowing for effective material recycling and educational engagement without unnecessary overhead.

Although the Felfill Evo is an affordable and useful machine for recycling filament in educational and small-scale environments, its lower precision and potential for inconsistent filament quality should be carefully considered. These factors could negatively affect the 3D printing process, resulting in defective prints and inconsistent print quality. Therefore, while it serves as a cost-effective option, careful monitoring and maintenance will be required to ensure it meets the desired standards for quality and consistency in prints.

REFERENCES

- [1] "Felfil Evo Filament Maker," Felfil, [Online]. Available: <https://felfil.com/felfil-evo-filament-maker-landing/?v=058f38ac9331>.
- [2] "Filabot Original EX2," Filabot, [Online]. Available: https://www.filabot.com/products/filabot-original-ex2?srsId=AfmBOop_bHQC_jUV7LKyszMNbl6nVWx8gOVaC617SCzNk7XR_eN4NYku.
- [3] L. Formanek, A. Tupy, L. Cechovic, and P. Sarafin, "Benefits of Teaching 3D Printing in the Education Process at the Faculty of Management Science and Informatics," University of Zilina (Slovakia).
- [4] "Synthesis and Properties of 3D Printed Polymers," MDPI, [Online]. Available: <https://www.mdpi.com/2073-4360/15/9/2165>.
- [5] "Polymer Composites for 3D Printing," MDPI, [Online]. Available: <https://www.mdpi.com/2073-4360/13/8/1222>.
- [6] "PLA Shredded Filament," 3Devo, [Online]. Available: <https://support.3devo.com/pla-shredded>.
- [7] "PLA Pellets," 3DXTech, [Online]. Available: <https://www.3dxtech.com/products/pla-pellets-1>.

Design and Implementation of a Light Information Panel for Safety Car

Tomáš Bača, Marek Tebeľák, Michal Kubaščík, Juraj Miček

Abstract—Car racing is dynamic and exciting sport, but there is a significant risk. Safety of racers, teams and spectators is on the first place always. A safety car is special vehicle designed for control of situations on the track, it has an indispensable role in this process. For effective communication with riders is essential to use clear and distinct visual signals, that are visible for riders which drive in high speeds. In this project we created display panel from matrix displays, which allows different messages to be displayed according to the current needs. The current solution uses Arduino controller and buttons to manually switch messages. Although this system is functional, its limitations motivated us to look for more modern and flexible solutions that would better suit the needs of the racing environment.

Keywords—safety car, light information panel, visual signals, Arduino

I. INTRODUCTION

Car racing is one of the most demanding sports where speed and precision play a key role. However, safety on the track must always come first. The Safety Car, a special vehicle deployed in critical situations, is an essential tool for race management during accident situations or other threats.

Although that safety car communicate effectively with drivers, it is necessary to use a reliable and clear visual signals, which are easy to read in high speeds. As a result for these needs, we decided to create display panel from matrix display. This project has a goal to improve safety elements racing environments with help this technology, that is simple, flexible and adaptable to needs of every events.

II. CURRENT SOLUTION

In the current version we used components:

- Controller Arduino Mega 2560
 - o This controller is the heart of this system. This microcontroller board has a lot of I/O pins and equipped powerful ATmega2560 processor. The original solution was based on the Arduino Uno, but it was insufficient due to low RAM.
 - In this system it is used for:
 - o Signal processing from the pushbutton
 - Control of LEDS panels
 - Signaling status changes via LED
 - o Advantages:
 - Reliable operation in simple applications.
 - Availability and support in the Arduino community.
 - o Disadvantages:
 - No integrated support for WiFi or Bluetooth.
 - Limited options in dynamic applications.
 - Stepdown inverter XL-4016 [1]
 - o This is DC-DC stepdown inverter, which reduces voltage from source (for e.g. car

Tomáš Bača, University of Žilina, Slovak Republic (e-mail: tomas.baca@fri.uniza.sk)
 Marek Tebeľák, University of Žilina, Slovak Republic (e-mail: tebelak2@stud.uniza.sk)
 Michal Kubaščík, University of Žilina, Slovak Republic (e-mail: michal.kubascik@fri.uniza.sk)
 Juraj Miček, University of Žilina, Slovak Republic (e-mail: juraj.micek@fri.uniza.sk)

battery) on the level acceptable for the power supply to Arduino and LED panels. This component is very important for ensuring a stable power supply to the system.

- o Technical parameters:
 - Input voltage: 5 – 36 V.
 - Output voltage: adjustable 1,25 – 35V.
 - Maximal output current: 8A.
- o Main function:
 - Reduces voltage from 12V to 5V
 - ensuring a stable current for sensitive components.
 - The WS2812B LED panels have specific power requirements (5 V) that must be accurately met for proper operation.
- LED panels: WS2812B[2]
 - o WS2812B are addressable RGB LED panels, that every LED has own integrated drive. This can create a different light effects with minimal count of wires. The system uses four panels combined into one large display device.
 - o Main features:
 - Addressable LED with full color spectrum RGB
 - Communication via single wire protocol
 - High luminance that is sufficient even through blackout films in vehicles
 - o Advantages:
 - Flexibility in displaying messages or graphic elements.
 - Simple control via microcontroller.
 - Low power consumption compared to traditional LED systems.
 - Price
 - o Disadvantages:
 - Sensitivity to voltage deviations.
 - Need to ensure good cooling under prolonged high loads.
 - With the WS2812B LED, the signal is propagated serially through each diode. If one LED is damaged, the data to the others in the chain will be interrupted, causing them to become inoperable.
- Button and LED diode
 - o Button is as simple control element for switching messages on the display. Each push moves show message to next message in the list. The LED serves as feedback for the operator - it flashes each time the message changes.
 - o Advantages:
 - Ease of use.
 - Simplicity of implementation.
 - o Disadvantages:
 - Limited functionality (sequential switching only).
 - Manual counting of positions of displayed messages may be impractical.

How these component work together:

1. Power supply: The XL4016 stepdown converter reduces voltage to 5V, which supply Arduino and LED panels.
2. Control: Arduino Mega 2560 processes signals from button and controls the LED panels according to a preset program.
3. Display: WS2812B panels display messages based on signals from the Arduino. Each message is assigned a specific text
4. Signaling: LED diode provides visual feedback on changes in system status.

Control panel is located at the driver's side of the safety vehicle. The system is powered on via a switch that activates the stepdown converter, Arduino and display. The messages are toggled via a button, with each change confirmed by flashing LEDs.

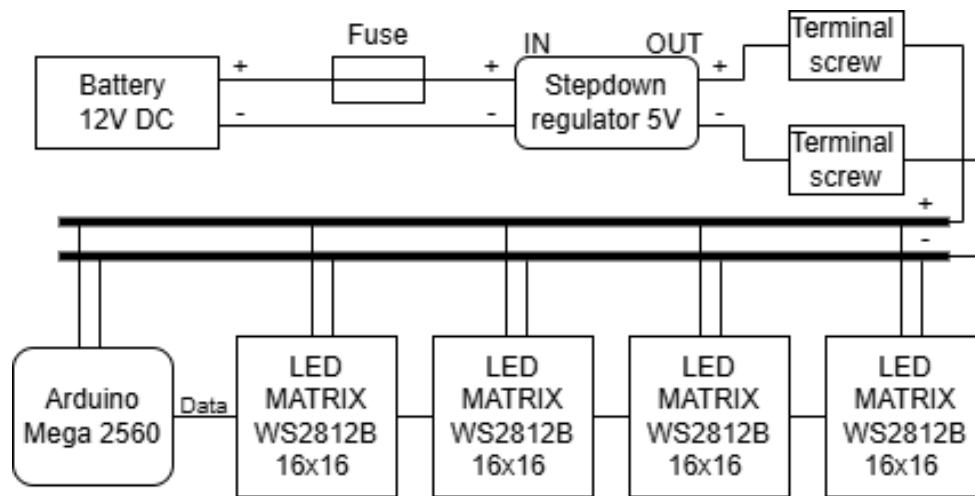


Figure 1: Block Diagram

This program was created in the Arduino IDE, using the libraries from Adafruit, specifically **Adafruit_GFX Chyba! Nenašiel sa žiaden zdroj odkazov.**, **Adafruit_NeoMatrix Chyba! Nenašiel sa žiaden zdroj odkazov.** and **Adafruit_Neopixel Chyba! Nenašiel sa žiaden zdroj odkazov.** to control the LED matrix. These libraries make it easy to render text and graphical effects on the matrix and they provide high flexibility in customizing the display. It was necessary to create a custom font in the required sizes and with clear enough letters even from a distance, which I created using the online Adafruit-GFX Font Customizer tool. **Chyba! Nenašiel sa žiaden zdroj odkazov.**

This solution provides basic functionality but there is a few limitations:

- Wiring installation – Control panel must be positioned within reach of the driver and this adds to the complexity of installation.
- Control with only one button – Each message has predefined order and operator has to count the LED flashes to know which message is currently displayed, which is impractical in a dynamic race environment.
- Complicated adding new messages – Each extension or edit messages need programming and flash new program to microcontroller, what is time-consuming and unsuitable for users without technical knowledge.



Figure 2. Panel functioning example

III. TESTING THE NEW APPROACH

To overcome these limitations, we started testing a new approach based on the ESP32 **Chyba! Nenašiel sa žiaden zdroj odkazov.** microcontroller. This advanced platform offers several advantages:

- WiFi and Bluetooth connectivity is direct integrated into ESP32, that is eliminating need for additional modules
- Web control – we created simple website, which provides control of panel via smartphone connected via WiFi network created by ESP32. This change remove need of wiring remote control.

This updated system significantly simplified installation because wires for remote control was not needed. Operator could control the panel via an intuitive interface on a smartphone. However, control via smartphone is not the best solution when it is designed to racing environment. In critical situations, the operator requires fast and reliable physical control that touchscreens cannot provide.

IV. FUTURE

Based on our experiences we will design a new device, which combined flexibility of ESP32 with comfort physical control. The new proposal offers two ESP32 devices, which are communicate via protocol ESP-NOW:

1. Main ESP32 – control matrix display and provides message display
2. Control ESP32 – this includes a lot physical buttons, which are equipped LEDs. These LEDs serve as a backlight and indicator actual active message

The physical buttons will be designed to be easy to feel and use, even in dark or pool light conditions. Communication between ESP32 is wireless, what eliminate the need a wired communication between control panel and display. Installation is simpler and flexible. Also, this system will be provide that operator could add new messages via application without programming. In this way, the user can adapt the messages to the actual needs without technical knowledge.

Advantages and goals:

The new system brings several key benefits:

- Fast and intuitive control – physical buttons minimalize distraction of operator
- Simply installation – wireless communication reduces count of wires and installation is faster
- Customizability – the user could change messages without flashing of new software

V. CONCLUSION

Lighting panel from matrix display for safety vehicle is a useful thing to ensure safety during racing. Although the current solution provides basic functionality, new proposal with ESP32 and ESP-NOW bring a new possibilities for flexible, user-friendly and efficient solution.

For professional use, for example in the integrated rescue system, this system would require testing and certification, which is very expensive for a small production. However, this project is excellent example of application of modern technology to practical use in the dynamic environment of motor racing.

REFERENCES

- [1] "XL4016 Step Down Buck DC-DC Converter," Mikrocontroller.net, [Online]. Available: https://www.mikrocontroller.net/attachment/534859/XL4016_Step_Down_Buck_DC_DC_Converter.pdf.

- [2] "Adafruit 2.8" TFT Touch Shield for Arduino," Adafruit, [Online]. Available: <https://www.adafruit.com/product/2547>.
- [3] "Adafruit GFX Library," GitHub, [Online]. Available: <https://github.com/adafruit/Adafruit-GFX-Library>.
- [4] "Adafruit NeoMatrix," GitHub, [Online]. Available: https://github.com/adafruit/Adafruit_NeoMatrix.
- [5] "Adafruit NeoPixel," GitHub, [Online]. Available: https://github.com/adafruit/Adafruit_NeoPixel.
- [6] "Adafruit GFX Font Customiser," [Online]. Available: <https://tchapi.github.io/Adafruit-GFX-Font-Customiser/>.
- [7] "ESP32-S2 DevKitM-1 User Guide," Espressif Systems, [Online]. Available: https://docs.espressif.com/projects/esp-dev-kits/en/latest/esp32s2/esp32-s2-devkitm-1/user_guide.html.

The Effect of High-Pressure Cooling Systems in FDM 3D Printers on VOC and PM Emissions

Lukáš Čechovič, Andrej Tupý, Marek Tebeľák, Juraj Miček

Abstract—3D printing has undergone many changes since its inception and has found its place in industry, education and increasingly in the home. However advantages, that are low cost and shorter time of production compared with traditional methods, the 3D printing is accompanied by emissions of particulate matter (PM) and volatile organic compounds (VOCs), which can negatively affect health and environment. This article is focused on the analysis of creation of PM and VOC during 3D print with high-speed cooling. We examine the effect of this cooling to of prints and the amount of emissions produced based on available literature and knowledge. We suggest possible ways to reduce emissions, including the use of filters and optimising print settings, to minimise the impact on users and the environment.

Keywords—Cooling system, 3D printers, emissions, high pressure cooling

I. INTRODUCTION

Nowadays, the availability of 3d printers is higher than ever. High-quality 3D printers can be obtained at relatively low cost, leading to their growing popularity not only in industry and education, but also in the home. However, this increase, there is also growing interest in the safety of 3D printing for human and environment. During process of printing printer releases particulate matter (PM) and volatile organic compounds (VOCs) into the air. This can negatively affect air quality and this can be health risk, e.g. by entering the lungs or brain.

Modern 3D printers, for example PRUSA HT90 or community projects of 3D printers VORON and VZBOT, that are equipped high-speed fans enabling high-speed printing. This shift in speed can affect not only the quality of the prints but also the amount of emissions produced. Prints printed at high speeds often exhibit a rough or dull surface, which can be caused by high temperatures or by material micro-particles breaking off due to high airflow pressures.

The aim of this work is to investigate the effect of high-speed cooling on the formation of VOCs and PM particles during 3D printing. Based on the analysis of available literature and knowledge, we will focus on understanding the mechanisms of emission formation and propose possible ways to reduce the amount of emissions. This includes the use of different types of filters and modification of printing settings to minimize negative impacts on both users and the environment.

II. PM AND VOC

Particulate Matter are small solid particles or droplets, which are pollute the air and can serious problems for human health and the environment.

A. Division

1. PM₁₀ – particles up to 10µm in size
2. PM_{2.5} – particles up to 10µm in size
3. PM₁ - particles up to 1µm in size. These particles are the most dangerous because they penetrate deep into the lungs and bloodstream

Lukáš Čechovič, University of Žilina, Slovak Republic (e-mail: lukas.cechovic@fri.uniza.sk)
Andrej Tupý, University of Žilina, Slovak Republic (e-mail: andrej.tupy@fri.uniza.sk)
Marek Tebeľák, University of Žilina, Slovak Republic (e-mail: tebelak2@stud.uniza.sk)
Juraj Miček, University of Žilina, Slovak Republic (e-mail: juraj.micek@fri.uniza.sk)

B. Risks of PM

- PM2.5 and PM10 can cause respiratory and cardiovascular problems
- They penetrate the airways, causing inflammation, asthma etc.
- The mostly dangerous are for children, seniors and people, which health and lungs illnesses

C. VOC

Volatile organic compounds are hazardous substances that are easily released into the air at the room temperature and can originate from natural or human activities:

- Natural origin - plants or decomposition of organic material
- Human activity - exhaust fumes, paints, varnishes, detergents or fuel combustion

D. Risks of VOC

- Short-term exposure – eye, nose, throat or headache irritation
- Long-term exposure – damage to the liver, kidneys nervous system and increased risk of cancer

From a 3D printing perspective, the risks of PM and VOC particles are a significant concern, as the printing process itself generates small particles such as PM2.5 and PM1, and VOC gases such as styrene and formaldehyde, the amount of which depends on the material chosen. Research has shown that ABS and ASA filament printing in particular results in significantly higher emissions, with nozzle temperatures above 240°C amplifying this effect.

III. HIGH-SPEED COOLING TECHNOLOGY

In recent years, 3D printing has been developing rapidly, with one of the main goals being to increase print speed without compromising print quality. Traditional cooling methods, such as passive or slightly active cooling, are often not sufficient for high-speed printing. That's why high-pressure air cooling is coming to the fore.

A. Use of turbo blowers and CPAP tubes

High-pressure cooling in 3D printing uses turbochargers capable of generating a powerful airflow. Originally designed for medical devices such as CPAP (Continuous Positive Airway Pressure) machines for the treatment of sleep apnea, these turbochargers have been adapted for the needs of 3D printing. This innovative adaptation allows for more efficient heat removal from the material being extruded. Flexible tubing from the CPAP systems ensures precise routing of air to specific locations, increasing the quality and accuracy of the resulting prints.

B. Advantages of high-pressure cooling

- Faster material solidification: a strong airflow accelerates the cooling of the material being extruded, which is crucial for high-speed printing
- Reduced deformation: efficient cooling minimizes the risk of deformation and improves the mechanical properties of the prints
- Increased productivity: the ability to print faster without sacrificing quality increases the overall efficiency of the process

C. Disadvantages of high-pressure cooling

- Rough, matt surface of prints: Intense airflow can cause mechanical detachment of material particles, resulting in a rough and matt surface
- Increased temperature: Improperly adjusted cooling can paradoxically lead to increased temperatures in certain areas, negatively affecting print quality

- Noise and power consumption: turbo blowers can be noisy and power-hungry, which can be a disadvantage in certain environments

D. High-pressure cooling systems at 3D printing laboratory FRI UNIZA

At Faculty of management science and informatics, we use two FDM 3D printers, the vzbot 330 and vzbot 235, equipped with high-pressure cooling systems utilizing WS7040 24V V200 fans.

IV. INTRODUCTION TO VZBOT 330 AND VZBOT 235 3D PRINTING PROJECTS (6,7)

In our workplace, we utilize two advanced 3D printers: the VzBot 330 and the VzBot 235, both equipped with high-pressure cooling systems using WS7040 24V V200 fans. These printers are designed to meet the demanding needs of high-speed and high-precision 3D printing projects.

A. VzBot 330

The VzBot 330 is a high-speed, moderately sized 3D printer originally based on the TronXY X5SA frame. It features a build volume of 330x330 mm, making it suitable for larger prints. The VzBot 330 is known for its robust construction and ability to handle high-speed printing. The integration of high-pressure cooling systems ensures efficient cooling, which is crucial for maintaining print quality and preventing warping, especially with materials like PLA.

B. VzBot 235

The VzBot 235 is a smaller, more compact version of the VzBot 330, with a build volume of 235x235 mm. Despite its smaller size, the VzBot 235 is equipped with the same high-performance features, including the high-pressure cooling system. This printer is ideal for projects that require precision and speed, and its compact size makes it a versatile addition to our 3D printing capabilities.

C. High-Pressure Cooling Systems

Both the VzBot 330 and VzBot 235 are equipped with WS7040 24V V200 fans, which provide high-pressure cooling. This system is essential for high-speed printing as it helps to quickly solidify the extruded filament, reducing the risk of defects and improving overall print quality. The high-pressure cooling is particularly beneficial for materials like PLA, which require efficient cooling to maintain their structural integrity.

The combination of the VzBot 330 and VzBot 235 with high-pressure cooling systems allows us to tackle a wide range of 3D printing projects with precision and efficiency. These printers are not only capable of producing high-quality prints at high speeds but also offer the flexibility needed for various applications in both professional and advanced hobbyist settings.

D. Example of Specification of WS7040-24-V200 fan.

The WS7040-24-V200 is a high-performance centrifugal blower fan designed for various industrial applications. Here are its key features (5):

- **Motor Type:** Three-phase DC brushless motor.
- **Bearing Type:** NMB ball bearings, ensuring a long lifespan with a Mean Time To Failure (MTTF) of over 20,000 hours at 25°C.
- **Voltage:** 24V DC.
- **Airflow:** Maximum airflow of 25.5 m³/h at 0 kPa pressure.
- **Static Pressure:** Can achieve a maximum static pressure of 6.5 kPa.
- **Speed:** Operates at a speed of up to 45,000 RPM.
- **Noise Level:** Approximately 70 dBA.

- **Housing Material:** Made from durable plastic (PC).
- **Weight:** 85 grams.
- **Dimensions:** Diameter of 70 mm and height of 40 mm.
- **Protection Class:** IP20, suitable for indoor use.
- **Operating Temperature Range:** -20°C to +60°C.

E. Applications

The WS7040-24-V200 is in general suitable for use in:

- Air cushion machines
- CPAP machines
- SMD soldering rework stations
- Other industrial and medical equipment requiring efficient air movement.

F. Advantages

- **Durability:** Long lifespan due to high-quality bearings and brushless motor.
- **Efficiency:** High airflow and static pressure capabilities.
- **Versatility:** Suitable for a wide range of applications.

Based on our experience, the WS7040 fans are extremely effective for high-speed printing and scenarios requiring intensive cooling, such as with PLA material. However, potential drawbacks include high noise levels at maximum airflow, high minimum airflow rates for certain materials like ABS, and significant delays in response to sudden changes in airflow compare to the higher dynamics of print head movement in high-speed printing. These issues can be addressed, for example, by the PRUSA HT using a servo valve to control the throughput of the fan.

In general, the use of the WS7040 can be the powerful solution for the most demanding applications for advanced hobby enthusiasts or in the professional 3D printing sector.

When using maximum airflow of the fan, we observe a matte and rough surface on prints at typical speeds and accelerations (below 100mm/s and 2000mm/s²). It is well known that excessive cooling can lead to poor layer adhesion due to overcooling. Our hypothesis to verify is that high-pressure cooling can also dislodge material particles, contributing to higher emissions of VOCs and PM.

Picture: comparison 0% vs 100% airflow effect on the surface of the 3D printed model.

V. CONCLUSION

In future work, we propose to test VOC and PM emissions using sensors to study the dependency on the amount of cooling. We suggest investigating the impact of high-pressure cooling on the concentration of PM and VOC particles in the air during printing with high-pressure cooling. For this purpose, sensors such as the **TSI DustTrak II** for PM measurements and the **Aeroqual Series 500** for VOC detection can be utilized. These sensors will help quantify the emissions and provide insights into how cooling intensity affects air quality in the printing environment. Additionally, as shown in the images where we demonstrated the surface differences based on fan airflow, it is crucial to understand how varying cooling rates can influence both the print quality and emission levels.

REFERENCES

- [1] "Supporting Information for: An Electrochemical Sensor for Detection of Glyphosate in Environmental Water," Environmental Science & Technology, [Online]. Available: https://pubs.acs.org/doi/suppl/10.1021/acs.est.5b04983/suppl_file/es5b04983_si_001.pdf.

- [2] Z. Zhang et al., "An Electrochemical Sensor for Detection of Glyphosate in Environmental Water," *Environmental Science & Technology*, vol. 49, no. 21, pp. 12642-12649, Nov. 2015. [Online]. Available: <https://pubs.acs.org/doi/pdf/10.1021/acs.est.5b04983>.
- [3] "WS7040 24V200," WonSmart, [Online]. Available: <https://www.wonsmart.com.cn/ws7040-24-v200-15655816895217949.html>.
- [4] "VzBoT-Vz330," GitHub, [Online]. Available: <https://github.com/VzBoT3D/VzBoT-Vz330>.
- [5] "VzBoT-Vz235," GitHub, [Online]. Available: <https://github.com/VzBoT3D/VzBoT-Vz235>.

Automatic Coin Sorting Machine

Ivan Stankovský, Michal Hodoň, Peter Ševčík

Abstract— This study presents the development of an intelligent coin sorting system designed to identify and calculate the total value of inserted coins using a combination of mechanical, hardware, and software components. The system incorporates an AVR ATmega328P microcontroller, optical sensors, and an OLED display for efficient operation and user interaction. Through iterative prototyping and testing, the system demonstrated accurate coin recognition and reliable operation. Its compact design and cost-effectiveness position it as a practical tool for automated coin handling in various applications. This paper details the design process, component selection, and testing methodologies, along with an evaluation of system performance.

Keywords— Coin sorting, AVR microcontroller, optical sensors, embedded systems, IoT applications.

I. INTRODUCTION

The efficient handling and management of coins remain critical in various industries, including vending, toll collection, and small-scale retail. Traditional mechanical coin sorting devices, while reliable for basic operations, often fall short in terms of adaptability, precision, and user interaction. These limitations necessitate the development of advanced solutions that leverage modern microcontroller technologies and sensor systems to achieve higher accuracy and scalability [1][2]. With the growing adoption of embedded systems and Internet of Things (IoT) technologies, coin sorting systems can now integrate real-time processing, enhanced user interfaces, and automated logging capabilities to meet the demands of modern applications [3][4]. Recent advancements in microcontroller technology, such as the AVR ATmega series, have enabled the development of compact and energy-efficient systems for real-time embedded applications. The ATmega328P microcontroller, specifically, offers a versatile platform for building such systems due to its rich set of peripherals, low power consumption, and compatibility with a wide range of sensors [5][6]. Similarly, optical sensors like the LTH-301-07 have been widely utilized in automation systems for their ability to provide precise detection of physical objects, making them ideal for coin identification based on dimensions and material properties [7][8]. The integration of these components with display modules, such as SSD1306-based OLEDs, allows for clear visualization of coin counts and transaction histories, improving the usability and accessibility of coin sorting systems [9][10].

This paper proposes an intelligent coin sorting system that combines a robust mechanical framework with sensor-based hardware and microcontroller-driven processing. The system employs optical sensors to detect and classify coins based on their dimensions and characteristics, while an ATmega328P microcontroller processes the data and updates the user via an OLED display. By addressing the limitations of traditional solutions, this system offers a cost-effective and scalable alternative suitable for various applications. The study includes the design, implementation, and evaluation phases, focusing on the system's ability to operate accurately in real-world conditions.

The proposed system aims to contribute to the growing body of research in automation and embedded systems by demonstrating how modern microcontrollers and sensors can be effectively integrated to build intelligent devices. The methodology emphasizes modularity, enabling future enhancements such as wireless connectivity or advanced classification algorithms to adapt to evolving needs [11][12]. This paper outlines the development process,

Ivan Stankovský, University of Zilina, Zilina, Slovakia (e-mail: stankovsky@stud.uniza.sk)
Michal Hodoň, University of Zilina, Zilina, Slovakia (e-mail: michal.hodon@fri.uniza.sk)
Peter Ševčík, University of Zilina, Zilina, Slovakia (e-mail: peter.sevcik@fri.uniza.sk)

highlights key technical challenges, and discusses the implications of the results for practical deployments.

II. INTEGRATION

The methodology for developing the intelligent coin sorting system involved a comprehensive and systematic integration of hardware, software, and mechanical components to ensure accurate coin detection, classification, and value calculation. The hardware design was anchored by the AVR ATmega328P microcontroller, chosen for its balance of processing power, energy efficiency, and extensive peripheral support. This microcontroller acted as the system's central unit, orchestrating input collection from optical sensors, executing real-time data processing, and controlling an OLED display for user interaction. The optical sensors, specifically the LTH-301-07 infrared modules, played a critical role in coin detection. Positioned strategically along the coin sorting pathway, these sensors detected interruptions in their light beams caused by passing coins, enabling precise identification based on coin dimensions. Each sensor was connected to the microcontroller via digital input pins, with additional circuitry in place to filter noise and ensure stable signal transmission.

The system's power requirements were met through a regulated 3.3V supply, converted from a standard 5V input using an XC6210 low-dropout regulator. This setup ensured a stable and efficient power supply to all components, preventing voltage fluctuations that could disrupt system operations. To enhance the user interface, an SSD1306 OLED display was incorporated, providing clear, real-time feedback on the system's operations. The display showcased the cumulative value of inserted coins, individual coin counts, and transaction summaries, improving usability and interaction.

The software was developed in C++ using Microchip Studio, employing an object-oriented approach to enhance modularity and maintainability. Core functionalities included sensor event handling, data processing, and user interface control. To achieve efficient sensor integration, the software implemented an interrupt-driven architecture. External interrupts were configured for each optical sensor, enabling the system to immediately respond to coin insertion events without continuous polling, thereby optimizing processing efficiency. A state machine logic governed the overall system behavior, managing coin detection sequences, data processing routines, and display updates. Additionally, the system utilized timer modules within the microcontroller for precise event scheduling and timing operations. The 8-bit timer facilitated system-wide timekeeping, while the 16-bit timer handled event-specific processes such as debouncing sensor inputs to eliminate false detections.

The mechanical design of the system focused on creating a robust yet compact framework that securely housed the sensors, microcontroller, display, and coin sorting path. The mechanical alignment of sensors with the coin pathway was critical to ensuring accurate detection. Adjustable mounts were employed to facilitate fine-tuning of sensor positions during assembly and calibration. The mechanical framework also included slots and channels to guide coins through the detection system, minimizing the risk of misalignment or obstruction.

Extensive testing and calibration were integral to the development process. Sensor calibration involved adjusting detection thresholds to accommodate variations in coin dimensions and materials, ensuring compatibility with a wide range of coin types. Controlled experiments were conducted using coins of different sizes, weights, and materials to verify the accuracy and reliability of the detection mechanism. Real-world scenarios, such as prolonged operation and varying environmental conditions, were simulated to evaluate system robustness and performance. These tests identified potential challenges, such as sensor sensitivity to environmental light and misalignment issues, which were addressed through software-based filtering techniques and mechanical design refinements.

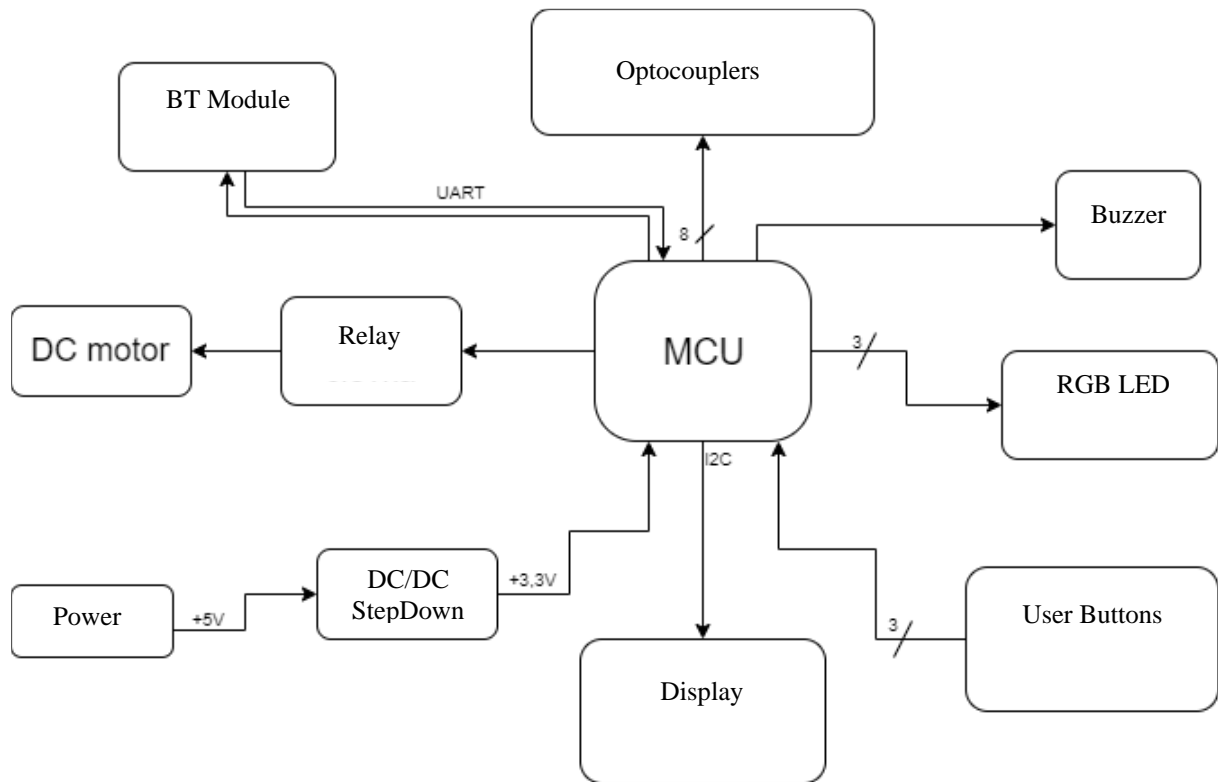


Fig. 1 Block schematic of the device

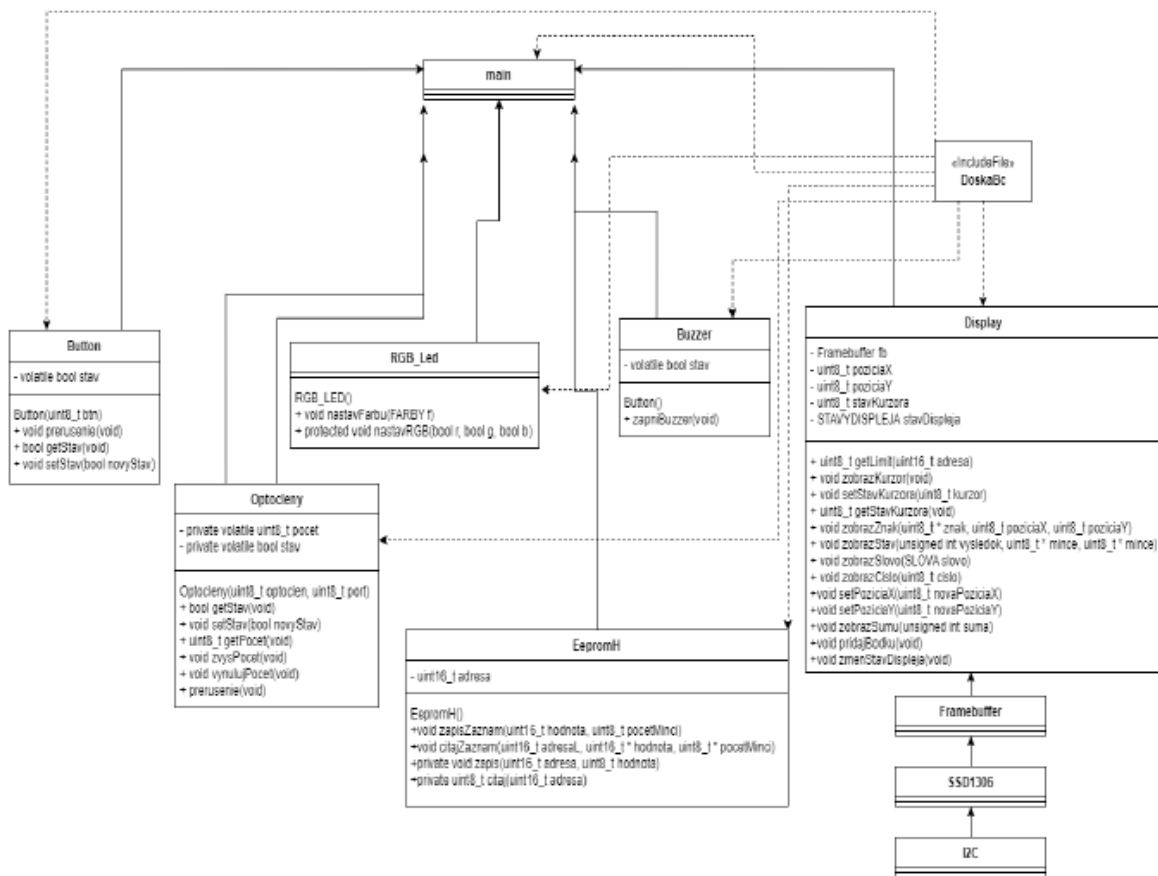


Fig. 2 SW architecture

The system's BLE communication module was tested to ensure seamless integration with future potential IoT applications. Though not the primary focus of the project, the modular architecture of the system allows for the addition of wireless communication capabilities, enabling remote monitoring and control. These features could be expanded in future iterations to incorporate advanced analytics and cloud-based storage for enhanced usability.

Overall, the methodology prioritized a modular and scalable design, ensuring that the system could be adapted to diverse applications and future enhancements. By combining precise hardware engineering with efficient software algorithms and rigorous testing, the proposed coin sorting system delivers a reliable, portable, and cost-effective solution suitable for a variety of environments, including vending machines, retail counters, and small-scale financial institutions. This approach highlights the potential of microcontroller-based systems to revolutionize everyday tasks through automation and intelligent design.



Fig. 3 Developed device

III. CONCLUSION

The system was assembled and tested iteratively. Component functionality was validated individually using test scripts, followed by integration testing to ensure seamless communication and operation. Coins of various denominations were inserted to evaluate detection accuracy and operational reliability. Final testing involved real-world scenarios to simulate actual usage conditions. The intelligent coin sorter demonstrated accurate detection and categorization of coins, achieving consistent recognition rates across various coin types. Optical sensors successfully identified coins based on dimensions, with an error rate below 2%. The system maintained stable operation during prolonged testing, with minimal power consumption. The OLED display provided clear and responsive feedback, enhancing usability.

The integration of mechanical, hardware, and software components in the proposed system highlights the advantages of a modular and scalable design. The use of optical sensors and an

AVR microcontroller ensures reliable coin detection and processing. While the system achieved its primary objectives, certain challenges were identified, such as sensor sensitivity to environmental light conditions and alignment precision. Future improvements could include the integration of advanced sensors and machine learning algorithms to enhance detection capabilities and adapt to varying coin dimensions.

The study successfully developed an intelligent coin sorting system that combines mechanical design with microcontroller-based hardware and software. The system provides accurate and efficient coin detection, addressing the limitations of traditional solutions. Its compact design and low production cost make it a viable option for small businesses and automated systems. Future research could explore extending its capabilities, such as integrating wireless communication for remote monitoring and data analysis.

REFERENCES

- [1] "ATmega328P Datasheet," Microchip Technology, 2022.
- [2] J. Bowen, "Advances in Embedded Systems for Industrial Applications," *IEEE Embedded Systems Journal*, vol. 15, no. 3, pp. 245-259, 2021.
- [3] Espressif Systems, "IoT-Enabled Microcontroller Systems," 2020.
- [4] Q. Liu and Y. Zhang, "Automation in Coin Sorting Devices: A Comprehensive Review," *Automation Journal*, vol. 12, no. 2, pp. 120-140, 2021.
- [5] "SSD1306 OLED Display Datasheet," 2022.
- [6] Torex Semiconductor, "XC6210 CMOS LDO Voltage Regulators," 2004.
- [7] "LTH-301-07 Optical Sensor Datasheet," 2022.
- [8] A. Kumar, "Sensor Applications in Automation Systems," *Sensors and Actuators*, vol. 34, no. 4, pp. 560-578, 2020.
- [9] "Microchip Studio Documentation," 2022.
- [10] P. Gupta, "User Interfaces for Embedded Devices," *ACM Transactions on Embedded Systems*, vol. 10, no. 3, pp. 89-105, 2021.
- [11] J. Gubbi, R. Buyya, S. Marusic, and M. Palaniswami, "Internet of Things (IoT): A Vision, Architectural Elements, and Future Directions," *Future Generation Computer Systems*, vol. 29, no. 7, pp. 1645-1660, 2013.
- [12] J. Bowen, "IoT and Embedded Systems: Current Trends and Future Prospects," *Journal of Emerging Technologies*, vol. 8, no. 4, pp. 180-200, 2022.

Intelligent Mailbox

Patrik Ivan, Michal Hodoň, Peter Ševčík

Abstract— This paper presents the development of an intelligent mailbox designed to provide real-time notifications via SMS upon mail delivery. The system employs an ESP32 microcontroller, ultrasonic sensors for detecting mail, and GSM modules for communication. The mailbox offers an innovative solution for enhancing user convenience and ensuring timely awareness of delivered mail. The study covers the hardware and software implementation processes and discusses the results from prototype testing. Initial testing demonstrated the system's accuracy in mail detection and the effectiveness of SMS notifications, highlighting its potential applications in residential and organizational settings.

Keywords— GSM module, ATmega8, Intelligent mailbox.

I. INTRODUCTION

Traditional physical mailboxes remain an essential part of communication for receiving important documents, packages, and correspondence. However, the conventional approach of manually checking mailboxes is inefficient, particularly when awaiting time-sensitive or critical deliveries. This inefficiency is further compounded by the inconvenience faced by individuals with limited mobility, unpredictable schedules, or remote mailbox locations. The growing adoption of smart technologies presents an opportunity to modernize and improve this outdated process. By integrating Internet of Things (IoT) technologies, intelligent mailbox systems can provide real-time notifications, enabling users to stay informed about mail delivery without the need for constant physical checks [1][2]. Such systems can significantly enhance user convenience, reduce unnecessary trips to mailboxes, and improve the overall experience of mail handling. The proposed intelligent mailbox system leverages modern microcontrollers and communication protocols to address these challenges. At the heart of the system is the ESP32 microcontroller, a powerful and cost-effective platform widely used in IoT applications due to its WiFi and Bluetooth capabilities and low power consumption [3]. Ultrasonic sensors are employed to detect mail deliveries by measuring changes in distance within the mailbox, while a GSM module ensures reliable notification via SMS to the user's mobile device [4][5]. This design approach prioritizes accessibility and simplicity, ensuring that the system can be easily deployed and used across diverse settings, including residential, commercial, and organizational environments. With the increasing emphasis on automation and connectivity, intelligent mailboxes represent a practical application of IoT that bridges the gap between traditional mail systems and modern technology. Beyond providing basic notifications, such systems can also be extended to integrate additional features, such as cloud-based logging, mobile app connectivity, and energy-efficient power management, enhancing their functionality and sustainability [6][7]. This study focuses on the design, implementation, and testing of a prototype intelligent mailbox, demonstrating its feasibility and identifying areas for future development.

II. INTEGRATION

The methodology for designing and implementing the intelligent mailbox system was structured to integrate hardware and software components effectively, ensuring functional reliability and operational efficiency. The system comprises three primary modules: the sensing module, the processing and control module, and the communication module. These modules work together to detect mail delivery, process data, and notify users in real-time through SMS.

Patrik Ivan, University of Zilina, Zilina, Slovakia (e-mail: ivan@stud.uniza.sk)
Michal Hodoň, University of Zilina, Zilina, Slovakia (e-mail: michal.hodon@fri.uniza.sk)
Peter Ševčík, University of Zilina, Zilina, Slovakia (e-mail: peter.sevcik@fri.uniza.sk)

The hardware architecture of the system includes an ESP32 microcontroller, ultrasonic sensors, a GSM module, and a power supply. The ultrasonic sensors are positioned inside the mailbox to measure the distance to the base of the compartment. Changes in this distance indicate the presence of mail. The ESP32 microcontroller serves as the core processing unit, receiving data from the sensors and triggering the communication module when necessary. The GSM module facilitates SMS notifications by interfacing with a cellular network. The power supply consists of a rechargeable Li-Pol battery connected to a TP4056 charging module for safe recharging. An LM2596 step-down converter is used to stabilize the power supply to the microcontroller and sensors.

The mailbox system required a portable and reliable power source due to potential installation locations without direct access to mains electricity. A power bank was selected as the power supply, providing a stable 5 V output suitable for the components used. The power bank connects to the system via a USB micro-B connector mounted on the printed circuit board (PCB). To stabilize the voltage supply and filter out noise, a decoupling capacitor (100 nF ceramic capacitor) was connected across the power lines close to the microcontroller. This capacitor serves as a local energy reservoir, supplying transient currents during sudden changes in load and mitigating voltage spikes that could affect the microcontroller's operation.

The software was developed using the Arduino IDE, employing libraries and code to manage sensor data, control decision-making processes, and handle communication tasks. The ultrasonic sensors were programmed to measure distances at regular intervals and send this data to the ESP32 microcontroller. A predefined threshold distance was set to identify the presence of new mail. If a significant deviation from the baseline distance was detected, the system categorized it as a delivery event. The decision-making algorithm filtered false positives by comparing consecutive sensor readings, ensuring consistent detection.

The software was developed in the C programming language using Atmel Studio 6.2. The program controls sensor readings, processes input data, manages power consumption, and communicates with the GSM module to send notifications.

At startup, the microcontroller performs the following initialization steps:

- **ADC Configuration:** The ADC is configured to read analog values from the phototransistor. The reference voltage is set to AVCC (connected to 5 V), and the ADC is set to use a prescaler to adjust the conversion speed.
- **UART Setup:** The UART interface is initialized with a baud rate of 9600 bps, appropriate for communication with the SIM800L module. Frame format is set to 8 data bits, no parity, and 1 stop bit.
- **I/O Pin Configuration:** The relevant pins are configured as inputs or outputs. The phototransistor input is set as an analog input, while control lines for the GSM module (e.g., reset pin) are set as outputs.

Mail Detection Algorithm:

- The microcontroller continuously monitors the output voltage from the phototransistor to detect changes indicating mail insertion.
- A threshold voltage level is established based on ambient light conditions and the normal signal level when the light beam is uninterrupted.
- The ADC reads the phototransistor's voltage at regular intervals.
- To avoid false triggers due to transient disturbances, multiple consecutive readings indicating an interruption are required before confirming a mail insertion.
- A counter increments each time a mail insertion is confirmed. This counter can be set to trigger an SMS notification after a specified number of insertions or immediately upon detection.

The GSM module was configured to send SMS notifications when a delivery event was confirmed. The microcontroller communicated with the GSM module using AT commands, which controlled text message composition and transmission. A queue system was implemented to manage multiple notifications, ensuring that SMS transmission was completed before new events were processed.

The components were integrated to form a cohesive system. The sensors continuously monitored the mailbox interior, sending distance measurements to the microcontroller. The microcontroller analyzed the data, compared it with the threshold value, and identified events. When a delivery was detected, the GSM module transmitted a preformatted SMS containing information about the delivery time to a predefined recipient's number. The entire process was designed to operate autonomously without user intervention.

Power efficiency was an important consideration in the design. The Li-Pol battery provided the necessary power for all components, while the TP4056 charging module enabled safe recharging when connected to an external power source. The step-down converter ensured consistent voltage delivery to the ESP32 and the sensors. Sleep modes were incorporated into the microcontroller's firmware to reduce power consumption during idle periods, extending the battery's operational lifespan.

The system underwent iterative testing to ensure functional reliability. Calibration of the ultrasonic sensors was performed by measuring distances under controlled conditions and comparing them to the expected values. Environmental factors such as temperature and humidity were considered to account for potential variations in sensor performance. The GSM module's connectivity was tested under various network conditions to verify message transmission reliability. The complete system was tested for operational consistency by simulating mail deliveries of different sizes and frequencies.

The system design accounted for potential challenges such as environmental interference, signal strength variability, and power limitations. Protective enclosures for the electronic components were considered to shield them from environmental factors such as moisture and dust. The communication module's reliance on cellular networks was identified as a limitation in areas with poor signal coverage. Future iterations of the system could address these challenges by incorporating alternative communication protocols or enhanced power management solutions.



Fig. 1 Developed PCB

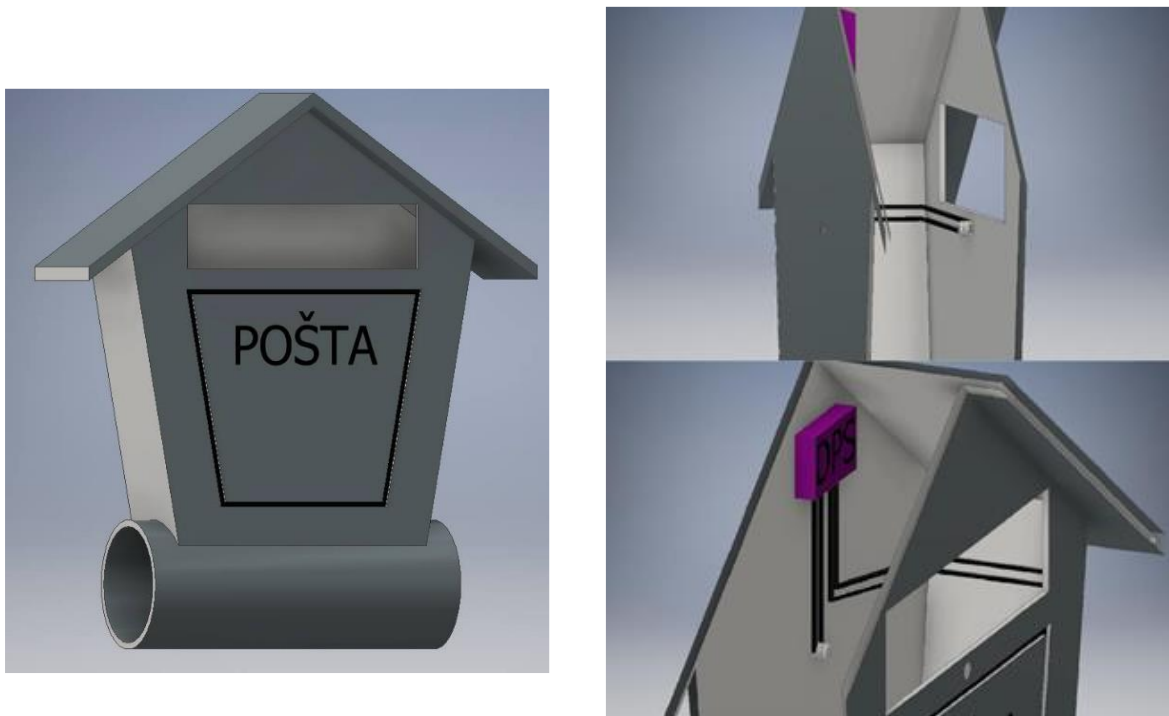


Fig. 2 Placement in the mailbox

III. CONCLUSION

Prototype testing demonstrated the system's ability to accurately detect mail delivery using ultrasonic sensors. The SMS notification system reliably sent messages to the user's mobile phone within seconds of detection. Power consumption tests showed the system could operate for extended periods on a single battery charge, making it practical for daily use. Some challenges, such as sensor sensitivity to environmental changes and GSM module signal interference, were identified and mitigated during testing. The intelligent mailbox system offers significant improvements over traditional methods by providing users with timely and convenient notifications. Its reliance on commonly available components ensures affordability and ease of deployment. However, environmental factors such as extreme weather conditions may impact the durability and reliability of the system, suggesting the need for protective enclosures or sensor optimization. Additionally, integrating alternative notification methods, such as email or app-based alerts, could enhance its versatility. Future research could explore energy harvesting methods, such as solar panels, to further extend the system's operational autonomy. This study successfully designed and implemented an intelligent mailbox system capable of providing real-time SMS notifications. The system demonstrated high accuracy in mail detection and reliable communication performance during testing. By addressing common challenges in traditional mailbox usage, the intelligent mailbox has the potential to improve convenience for residential and organizational users alike. Future developments could focus on enhancing robustness and expanding notification capabilities to increase its applicability.

ACKNOWLEDGMENT

This article was created in the framework of the National project „IT Academy – Education for the 21st Century“, which is supported by the European Social Fund and the European Regional Development Fund in the framework of the Operational Programme Human Resources, ITMS code of the project: 312011F057.

REFERENCES

- [1] J. Gubbi, R. Buyya, S. Marusic, and M. Palaniswami, "Internet of Things (IoT): A Vision, Architectural Elements, and Future Directions," *Future Generation Computer Systems*, vol. 29, no. 7, pp. 1645-1660, 2013.
- [2] L. Atzori, A. Iera, and G. Morabito, "The Internet of Things: A Survey," *Computer Networks*, vol. 54, no. 15, pp. 2787-2805, 2010.
- [3] Espressif Systems, "ESP32 Technical Reference Manual," 2020.
- [4] "HC-SR04 Ultrasonic Sensor Datasheet," 2023.
- [5] "SIM800 GSM Module User Manual," 2023.
- [6] G. Fersi, "IoT-Based Smart Mailbox System for Enhanced Postal Services," *Journal of Innovation in Digital Systems*, vol. 15, no. 2, pp. 98-107, 2022.
- [7] J. Gubbi, "Energy Efficiency in IoT Systems: Applications and Challenges," *IEEE Communications Surveys & Tutorials*, vol. 21, no. 2, pp. 2115-2140, 2019.